Children's drawings from Seiberg–Witten curves

SUJAY K. ASHOK, FREDDY CACHAZO AND ELEONORA DELL'AQUILA

We consider $\mathcal{N} = 2$ supersymmetric gauge theories perturbed by tree level superpotential terms near isolated singular points in the Coulomb moduli space. We identify the Seiberg-Witten curve at these points with polynomial equations used to construct what Grothendieck called "dessins d'enfants" or "children's drawings" on the Riemann sphere. From a mathematical point of view, the dessins are important because the absolute Galois group $\mathrm{Gal}(\overline{\mathbb{Q}}/\mathbb{Q})$ acts faithfully on them. We argue that the relation between the dessins and Seiberg–Witten theory is useful because gauge theory criteria used to distinguish branches of $\mathcal{N} = 1$ vacua can lead to mathematical invariants that help to distinguish dessins belonging to different Galois orbits. For instance, we show that the confinement index defined in hep-th/0301006 is a Galois invariant. We further make some conjectures on the relation between Grothendieck's program of classifying dessins into Galois orbits and the physics problem of classifying phases of $\mathcal{N} = 1$ gauge theories.

1. Introduction

The interest in $\mathcal{N} = 2$ supersymmetric gauge theories is especially due to the seminal work of Seiberg and Witten in the mid 90s [1,2]. They showed that the low-energy action and infrared dynamics of the gauge theory on the Coulomb branch can be completely solved and that all the relevant information about the low-energy theory is encoded in a hyperelliptic curve and in an associated meromorphic differential. This work led to a tremendous amount of progress in the understanding of the physical aspects of $\mathcal{N} = 2$ gauge theories, including the vacuum structure of related $\mathcal{N} = 1$ theories. At the same time, there have also been fascinating connections between Seiberg–Witten theory and mathematics, especially to the Donaldson theory of four manifolds [3].

In this article, we unearth a new connection between a particular class of Seiberg–Witten curves and what Grothendieck called "dessins d'enfants" or "children's drawings". We will refer to these simply as "dessins" in what follows. We will formally define a dessin later on, but for the moment by a dessin we simply mean a connected graph on a two-dimensional surface, with vertices of two kinds — say black and white — that alternate along the graph.

The original reason for studying such drawings in mathematics was that there is a natural action of the absolute Galois group $\mathrm{Gal}(\overline{\mathbb{Q}}/\mathbb{Q})$ on them. Moreover, the action is faithful, i.e., there is no group element, other than the identity, that leaves invariant all dessins. The absolute Galois group is one of the central objects of interest in mathematics, especially in number theory. Surprisingly, this object has already made its appearance in the physics literature in the context of rational conformal field theory due to work by Moore and Seiberg [4–6]. It has been known that the solutions of the Moore–Seiberg equations lead to a projective representation of the so called Teichmüller tower. As noted by Grothendieck in [7], the absolute Galois group also acts on this tower. Amusingly enough, both the Teichmüller tower and the dessins were introduced by Grothendieck in the same letter [7].

In the rest of Section 1 we will summarize recent progress made in [8, 9] in understanding the vacuum structure of $\mathcal{N} = 1$ gauge theories obtained by deforming an $\mathcal{N} = 2$ theory by a tree level superpotential. We will see that these gauge theory techniques and the existing results could have implications for the study of the action of the Galois group on the dessins and, conversely, we would like to argue that there is a wealth of information on the mathematical side that could potentially lead to an improved understanding of the phases of $\mathcal{N} = 1$ gauge theories.

More generally, we conjecture that there is an intimate relation between Grothendieck's program of classifying dessins into Galois orbits and the physics problem of classifying certain special phases of $\mathcal{N} = 1$ vacua. The precise form of the conjecture is given in Section 4.4. The meaning of the different physical and mathematical elements that go into this conjecture will be explained in the remaining part of Section 1 and in Section 2, respectively.

This paper is organized as follows: in Section 2, we discuss the dessins and related mathematical material. This includes Belyi maps, the action of $\mathrm{Gal}(\overline{\mathbb{Q}}/\mathbb{Q})$ on dessins via Belyi maps and the correspondence with Seiberg–Witten curves. In Section 3, we review the concept of invariants (order parameters) which are used to distinguish orbits of dessins under the action of $\mathrm{Gal}(\overline{\mathbb{Q}}/\mathbb{Q})$ ($\mathcal{N} = 1$ gauge theory phases). In Section 4, we give examples of cross fertilization that arise from our identification of the physics and mathematics programs. In particular, we explain how the confinement

index introduced in [8] leads to a Galois invariant. In Sections 5 and 6, we give some illustrative examples in full detail. In Section 7, we conclude with many open questions and directions for future work. In Appendix A, we give a very basic introduction to algebraic concepts in Galois theory with the goal of understanding the definition of $\mathrm{Gal}(\overline{\mathbb{Q}}/\mathbb{Q})$ and its action. In the same appendix, a small glossary of terms used in the text is given. Finally, in Appendices B and C, we expand on some interesting issues discussed in the rest of the paper.

1.1. Physics preliminaries

In the Seiberg–Witten solution of $\mathcal{N} = 2$ gauge theories, it is natural to study the loci in the moduli space where the SW curve develops singularities. For a pure $U(N)$ gauge theory — the most well-studied case — the curve has the form

$$(1.1) \qquad y^2 = P_N^2(z) - 4\Lambda^{2N} \,,$$

where $P_N(z) = \langle \det(zII - \Phi) \rangle$ and Φ is the adjoint scalar in the vector multiplet. (We adopt the usual notation, with the subscripts denoting the degree of the polynomials.) A well-studied [8] factorization is

$$(1.2) \qquad P_N^2(z) - 4\Lambda^{2N} = F_{2n}(z)\, H_{N-n}^2(z) \,,$$

which corresponds to a family of degenerate curves. Let us briefly discuss the physical information that is encoded in this kind of polynomial equation.

The $\mathcal{N} = 2$ Coulomb moduli space of the gauge theory is parametrized by N parameters $u_k = \frac{1}{k}\langle \mathrm{Tr}\Phi^k \rangle$, constructed from the adjoint scalar Φ. The problem studied in the physics literature is to find and classify the $\mathcal{N} = 1$ supersymmetric vacua obtained by perturbing the $\mathcal{N} = 2$ theory by a tree level superpotential

$$(1.3) \qquad W_{\mathrm{tree}} = \sum_{k=1}^{n+1} \frac{g_k}{k}\, \mathrm{Tr}\Phi^k \,.$$

Once the tree level potential is introduced, all points in the Coulomb moduli space are lifted except those for which $N - n$ mutually local magnetic monopoles become massless. The superpotential triggers the condensation of monopoles and the magnetic Higgs mechanism leads to confinement of the electric charges. The points at which this occurs are precisely those that solve the factorization problem (1.2). At low energies at these points, out of

the original $U(1)^N$ only a $U(1)^n$ subgroup remains unbroken and its coupling constants are given by the reduced Seiberg–Witten curve

$$(1.4) \qquad\qquad y^2 = F_{2n}(z).$$

From a simple counting of parameters, we see that (1.2) defines an n-dimensional subspace of the moduli space. Plugging the u_k's as functions of these n parameters into the superpotential W_{tree}, one gets an effective superpotential

$$(1.5) \qquad\qquad W_{\text{eff}} = \sum_{k=1}^{n+1} g_k \, u_k$$

on the moduli space. Thus, given the parameters g_k, one can vary with respect to the coordinates on the moduli space and obtain *all* the u_k's as functions of the g_k's and Λ.

In other words, the form of the superpotential picks out specific points in the $\mathcal{N} = 2$ moduli space which correspond to $\mathcal{N} = 1$ vacua. What was shown in [10, 11] is that this extremization problem can be rephrased as the problem of factorizing the Seiberg–Witten curve in the following manner:

$$(1.6) \qquad P_N^2(z) - 4\Lambda^{2N} = \frac{1}{g_{n+1}^2}((W'_{\text{tree}}(z))^2 + f_{n-1}(z)) \, H_{N-n}^2(z).$$

Let us denote the critical points of W_{tree} by a_i, i.e., $W'_{\text{tree}}(z) = \prod_{i=1}^{n} g_{n+1}$ $(z - a_i)$. We set $g_{n+1} = 1$ in what follows.

It is interesting to ask what the "moduli space" of $\mathcal{N} = 1$ vacua is, as the parameters g_k's are varied. The motivation for such a question was explained in [8]: semiclassically, as $\Lambda \to 0$, the gauge group $U(N)$ can be broken to $\prod_{i=1}^{n} U(N_i)$ with $\sum_{i=1}^{n} N_i = N$ by choosing Φ to be a diagonal matrix with N_i entries equal to a_i[1]. It is therefore natural to ask whether it is possible quantum mechanically to interpolate between vacua that have the same n but different N_i's.

This was answered in [8] where it was shown that, for example, vacua with one $U(1)$ factor can be smoothly connected to vacua with any allowed values of N_i's. All these classical limits are different corners of a single connected subspace of the $\mathcal{N} = 2$ moduli space, which was referred to as an $\mathcal{N} = 1$ branch. However, in [8] it was also discovered that there were other

---

[1] We assume that all $N_i \neq 0$. See Appendix C for some comments about the case when some of the N_i are zero.
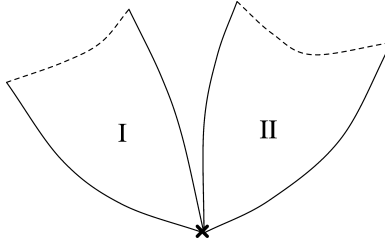
Figure 1: Two $\mathcal{N} = 1$ branches of the $U(4)$ gauge theory obtained by deforming the $\mathcal{N} = 2$ theory by a cubic superpotential. Only those branches with two $U(1)$'s in the infrared are shown. The two branches meet at a point where one more monopole becomes massless.

branches distinguished by order parameters such as the expectation values of Wilson loops. Branches meet at points where extra massless mutually local monopoles appear. At these points other, branches also emanate which have the same dimension but where some of the N_i's are zero.

The structure of these branches and how they meet can be quite intricate [8]. We use the example of a cubic superpotential in a $U(4)$ gauge theory to represent a region close to one of the points with three massless monopoles in figure 1. At a generic point, the low energy group is $U(1)^2$. At the special point where the two branches meet, a third branch (not drawn) emanates, which consists of vacua with a single $U(1)$ as the low-energy group. Along each of the depicted branches one can take a semi-classical limit and find vacua corresponding to (classically) unbroken $U(N_1) \times U(N_2)$ gauge groups.

1.2. Dessins from gauge theory

Let us continue our analysis of the $U(4)$ example. In figure 2, we show a typical configuration of the zeroes of the polynomials that appear in (1.2), which correspond to points in the branches shown in figure 1 near the semi-classical limits. The line segments that are drawn represent the branch cuts. Of course, it is not essential to draw the cuts through the zeroes of $P(z)$ (denoted by $\circ$) but this will have a mathematical significance when we formally define a dessin. On the other hand, the cuts naturally pass through the zeroes of $H_2^2(z)$ (denoted by a bivalent $\bullet$ node in the drawing) since a small deformation away from the $\mathcal{N} = 1$ branch will split the double zeroes. As is clear from the figure, these look like disconnected branchless trees.

It turns out that one of the two branches in figure 1 has $U(2) \times U(2)$ as the only semi-classical limit [8]. We now focus our attention on this branch. We
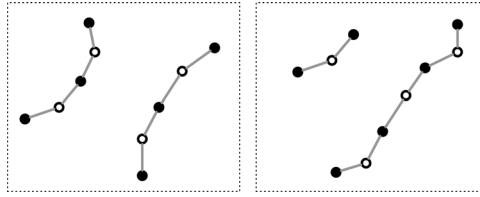
Figure 2: Zeroes of $P_4(z)$ (denoted by $\circ$), zeroes of $F_4(z)$ (denoted by univalent $\bullet$) and zeroes of $H_2^2(z)$ (bivalent $\bullet$) near the semi-classical limits with $N_1 = N_2 = 2$ (left) and $N_1 = 1$, $N_2 = 3$ (right). Edges represent branch cuts.

further tune the parameters of the superpotential so that the corresponding $\mathcal{N} = 1$ vacuum is an isolated singular point where $H_2(z)$ develops a double root. There is only one such point in the branch we have chosen and it naturally leads to a connected graph. This is shown in figure 3. We have omitted the zeroes of $P_4(z)$ so as to not clutter the figure.

It turns out that such connected trees show up in the moduli space whenever the Seiberg–Witten curve develops isolated singularities. Examples of such "rigid curves" include the maximally confining points [1, 12] and the generalized Argyres–Douglas points [13]. Such singularities arise when some of the zeroes of F_{2n} and H_{N-n} coincide, $F_{2n}(z)$ develops double roots, etc.

The connected trees that appear at such special points in the moduli space are precisely the "dessins d'enfants" that Grothendieck introduced as
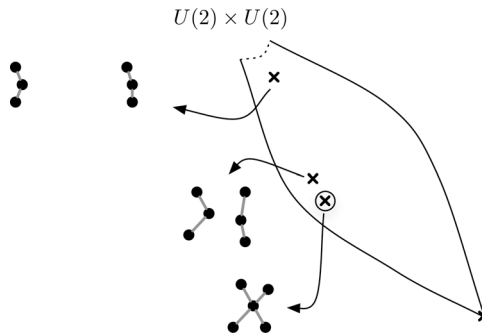

Figure 3: Evolution of the two branchless trees in one $\mathcal{N} = 1$ branch of the $U(4)$ gauge theory starting near the $U(2) \times U(2)$ semi-classical limit and reaching an isolated singularity where we get a connected tree.

a tool to study the structure of the absolute Galois group $\mathrm{Gal}(\overline{\mathbb{Q}}/\mathbb{Q})$. This is the group of automorphisms of $\overline{\mathbb{Q}}$ that leave $\mathbb{Q}$ fixed[2]. As mentioned earlier $\mathrm{Gal}(\overline{\mathbb{Q}}/\mathbb{Q})$ acts faithfully on the dessins. This means that the only element of the group that leaves every dessin invariant is the identity. The set of dessins is then partitioned into orbits under the action of the group. (We exhibit how $\mathrm{Gal}(\overline{\mathbb{Q}}/\mathbb{Q})$ acts on the dessins in Section 2.4.) One way of learning about the Galois group is to construct a complete set of invariants that distinguish dessins that belong to distinct Galois orbits. This is one of the goals in the study of dessins in mathematics and we will discuss some of the known Galois invariants in detail in Section 3.

In the following sections, we show that the known order parameters that distinguish different branches of $\mathcal{N} = 1$ vacua can be thought of as Galois invariants. In particular, we prove that the "confinement index" introduced in [8] is a Galois invariant and can be given a purely combinatorial interpretation. Interestingly, we will find that certain operations on the gauge theory side, such as the "multiplication map" introduced in [10], have a precise interpretation as operations on the dessins. We believe that solving the non-rigid problem in (1.2) before specializing to singular points might lead to a new and useful perspective in the study of dessins d'enfants. Conversely, we will also see that this correspondence leads to open questions regarding the interpretation of interesting mathematical invariants in the gauge theory.

More explicitly, we would like to argue that the special points where the dessins make their appearance can be thought of as special phases of the $\mathcal{N} = 1$ gauge theory. This would imply the existence of appropriate order parameters, which distinguish these special points from generic points in the $\mathcal{N} = 1$ branch to which they belong. We provide some evidence for this in the examples in Section 5.2.

So far, we have seen in an example how dessins can arise at isolated singular points in the moduli space of a Seiberg–Witten curve. We will now show that given a dessin, one can associate to it a polynomial equation which corresponds to a singular Seiberg–Witten curve, of the type discussed in this section. It turns out that this is precisely equivalent to the content of the Grothendieck correspondence, which we discuss next.

---

[2] Here, $\mathbb{Q}$ is the field of rational numbers and $\overline{\mathbb{Q}}$ is its algebraic closure. For more details, see Appendix A.

2. The Grothendieck correspondence

2.1. Mathematical preliminaries

The Grothendieck correspondence is a bijection between classes of dessins and special classes of maps on punctured Riemann surfaces called Belyi maps. At first sight, this might seem far removed from gauge theory physics but we will describe a precise route to arrive at the correspondence between Seiberg–Witten theory and the dessins d'enfants.

The first ingredient in the correspondence is the Belyi map. A Belyi map [14] is a holomorphic map from any punctured Riemann surface to $\mathbb{P}^1$ with exactly three critical values at $\{0, 1, \infty\}$. In [7], Grothendieck showed that any dessin can be constructed from a Belyi map. For the purposes of our discussion, we will restrict to dessins drawn on a Riemann sphere[3]. We show two simple examples in figure 4. The key result that makes explicit the relation to Seiberg–Witten theory is that Belyi maps are obtained as solutions to certain polynomial equations.

As we will see, these equations have a natural interpretation as Seiberg–Witten curves that describe particular degenerations of Riemann surfaces, such as those we have already encountered in the introduction. More generally, we find that whenever the Seiberg–Witten curve factorizes so as to give rise to a "rigid curve", i.e., without free parameters, one can associate a
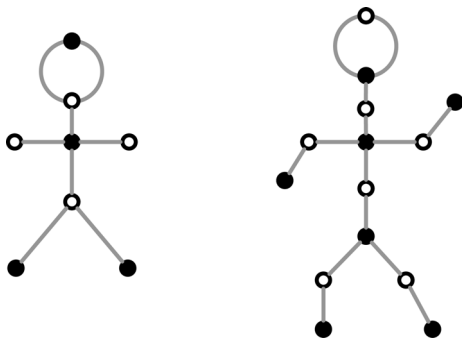

Figure 4: Examples of dessins; the bipartite structure of the graph is manifestly shown.

---

[3] All the mathematical discussion in this section can be generalized to a general Riemann surface and we refer the interested reader to [15].

dessin to it[4]. Our goal will be to set-up a dictionary that maps the relevant quantities in mathematics, related to the Galois group action on dessins, into gauge theory language and vice versa.

2.2. Dessins from Belyi maps

We now state without proof some basic mathematical facts, which are crucial to establish the relation between the dessins and Seiberg–Witten theory. See [15] for a thorough discussion and for a full list of references. The main result we will use is the Grothendieck correspondence, which connects the theory of dessins with algebraic curves defined over $\overline{\mathbb{Q}}$, the algebraic closure of $\mathbb{Q}$. Let us see how this comes about.

Consider an algebraic curve X defined over $\mathbb{C}$. Such a curve is defined over $\overline{\mathbb{Q}}$ if and only if there exists a non-constant holomorphic function $f : X \to \mathbb{P}^1$ such that all its critical values lie in $\overline{\mathbb{Q}}$. A theorem by Belyi [14] gives a very striking result: X is defined over $\overline{\mathbb{Q}}$ if and only if there exists a holomorphic map $f : X \to \mathbb{P}^1$ such that its critical values are $\{0, 1, \infty\}$.

A map $\beta : X \to \mathbb{P}^1$ with all its critical values in $\{0, 1, \infty\}$ is therefore called a *Belyi map*. A Belyi map is called *clean* if all ramification degrees over 1 are exactly equal to 2.

Let us give a simple example that will be very relevant in the rest of the paper. Let $X = \mathbb{P}^1$ and β a polynomial. To guarantee that all critical points that map to 1 have ramification degree 2, we set

$$(2.1) \qquad \beta(z) = 1 - P^2(z) \,,$$

where $P(z)$ is a polynomial. Let us see under which conditions β is a clean Belyi map. The critical points are computed as the zeroes of

$$(2.2) \qquad \frac{d\beta(z)}{dz} = -2P(z)P'(z).$$

This means that the zeroes of $P(z)$ are critical points. Their ramification degree is 2 since $P(z)$ is squared in β and their critical value, i.e., β evaluated at a zero of $P(z)$, is 1. All we need is that the remaining critical points, which are precisely the roots of $P'(z)$, have critical value 0. In other words, they must also be roots of $1 - P^2(z)$. Up to the freedom to shift z, these conditions have only a discrete number of solutions. These are Belyi maps.

---

[4] This is up to a shift of z in (1.2). In gauge theory, this corresponds to the overall $U(1)$ degree of freedom that decouples from the strong dynamics in the infrared.
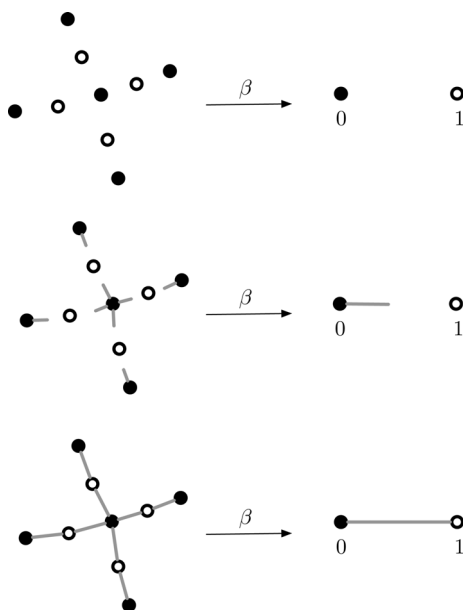
Figure 5: We show how the dessin is the pre-image of the interval $[0,1]$ under the Belyi map. Note that as we move from 0 to 1, the number of lines emanating from a given pre-image of 0 is given by the ramification degree of the map at those points. Since the map is clean, *exactly* two lines meet at each pre-image of 1.

We now have the ingredients to formally define a dessin: for the purposes of this paper, we define a *dessin d'enfant* on the sphere as the pre-image under a clean Belyi map of the interval joining 0 and 1 in $\mathbb{P}^1$. In other words, the dessin D associated to a clean Belyi map β is $D = \beta^{-1}([0,1]) \subset X$. We show this pictorially in figure 5 for the case $\beta(z) = 1 - P_4^2(z) = F_4(z)\,H_1^4(z)$.

Such a dessin has a natural bipartite structure given by assigning a • to the pre-images of 0 and ∘ to the pre-images of 1. We will refer to a pre-image of 0 as a vertex of the dessin. An edge is a line segment between two vertices that contain exactly one pre-image of 1. For example, the second dessin in figure 4 is clean (while the first is not) so that the notion of edges and vertices as we just defined makes sense: it has seven edges and seven vertices. In what follows, we will restrict our attention to clean dessins and refer to them simply as dessins. Likewise, the corresponding clean Belyi maps will be simply called Belyi maps.

Also important for characterizing the dessins are the pre-images of ∞, denoted by ×. There is one pre-image of ∞ for each open cell enclosed by a

set of edges. For example, a dessin is a tree if and only if the pre-image of ∞ is a single point.

The study of dessins on the sphere is important because the absolute Galois group $\mathrm{Gal}(\overline{\mathbb{Q}}/\mathbb{Q})$ acts faithfully on them. As mentioned before, the absolute Galois group is the group of automorphisms of $\overline{\mathbb{Q}}$ that leaves invariant $\mathbb{Q}$ and it is a remarkably complex object. We give a basic introduction to the Galois group in Appendix A. It can also be shown that not only is the action of $\mathrm{Gal}(\overline{\mathbb{Q}}/\mathbb{Q})$ on genus-0 dessins faithful, but so is the action on the much smaller set of trees.

The main thing to take away from this section is that one can map the problem of classifying dessins to the problem of classifying Belyi maps β. As we have seen, these are a special class of rational functions on the Riemann sphere that satisfy the conditions in the definition above. We now turn to the question of how Belyi maps corresponding to a given dessin can be explicitly constructed. This will naturally lead us to gauge theory physics.

2.3. Belyi maps from polynomial equations

Consider a dessin D on the sphere with N edges. Let $V = \{u_1, \ldots, u_k\}$, where u_i is the number of vertices (pre-images of 0) of valence i. We choose k to be the maximum vertex valence in D. Let $C = \{v_1, \ldots, v_m\}$, where v_i is the number of faces with i edges. Again we choose m to be the maximum face valence in D. The lists V and C are called the *valency lists* of D.

Let $G_{v_i}(z)$ and $J_{u_i}(z)$ be polynomials of degree v_i and u_i respectively, with undetermined coefficients. Take one polynomial for each element in V and in C. Pick i_0 to be the valence whose v_{i_0} is the smallest non-zero value in C. Then let all polynomials $G_{v_i}(z)$ and $J_{u_i}(z)$ be monic except for $G_{v_{i_0}}(z)$ which we choose to be of the form

$$(2.3) \qquad G_{v_{i_0}}(z) = \alpha(z^{v_{i_0}-1} + \cdots).$$

In other words, we have chosen the coefficient of $z^{v_{i_0}}$ to vanish and we have factored out the coefficient of $z^{v_{i_0}-1}$ which we call α.

Now construct the two polynomials

$$(2.4) \qquad A(z) = \prod_{j=1}^{k} J_{u_j}(z)^j, \quad B(z) = \prod_{i=1}^{m} G_{v_i}(z)^i.$$

Then if $A(z)$ and $B(z)$ are such that there exists a monic polynomial $P_N(z)$, with N equal to the number of edges of the dessin, and which satisfies the

polynomial constraint

$$(2.5) \qquad\qquad A(z) - B(z) = P_N^2(z),$$

then

$$(2.6) \qquad\qquad \beta(z) = 1 + \frac{P_N^2(z)}{B(z)} = \frac{A(z)}{B(z)}$$

is a rational clean Belyi map. Note that the polynomial equation is rigid, in the sense that there are no coefficients in the polynomials which are free parameters[5]. There are thus only a finite number of solutions to (2.4). The discussion has been rather abstract so far, so let us illustrate the various concepts with some simple examples which have already been discussed in [16].

Consider the dessin in figure 6 which has six edges. From the figure, we see that each open cell is bounded by three edges and every vertex is trivalent. The valency lists are therefore of the form $V = \{0, 0, 4\}$ and $C = \{0, 0, 4\}$. From the discussion above, we need $A(z) = J_4^3(z)$ and $B(z) = G_3^3(z)$ such that they satisfy the polynomial equation

$$(2.7) \qquad\qquad P_6^2(z) + G_3^3(z) = J_4^3(z).$$

It turns out that there is only one solution to the polynomial equation (2.7) [16]. However, in general, such polynomial equations have more than one solution. For instance, the polynomial equation

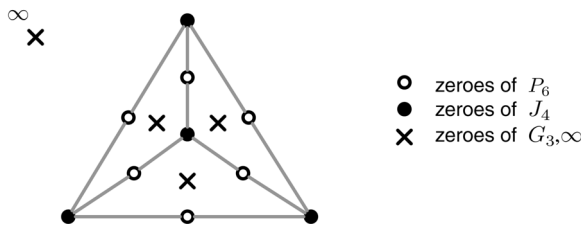$$(2.8) \qquad\qquad P_{10}^2(z) + G_3^5(z) = J_4^3(z)\, \widetilde{J}_4^2(z).$$

Figure 6: Dessin corresponding to the solution of the factorization problem (2.7).

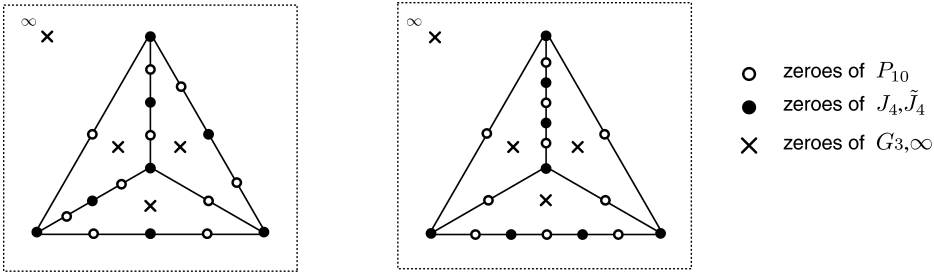[5] Up to a shift and rescaling of z. We will return to this point in Section 2.7.

Figure 7: Dessin corresponding to the solution of the factorization problem (2.8). The bivalent ● vertices are roots of $\widetilde{J}_4(z)$ while the trivalent ● nodes are the roots of $J_4(z)$.

turns out to have two solutions [16]. This is because for the same valency lists $V = \{0, 4, 4\}$ and $C = \{0, 0, 0, 0, 4\}$ (which we can infer from the polynomial equation), there are two dessins one can draw. These are shown below in figure 7. We shall revisit this specific example in Section 6 in much more detail.

The key result which we will use from now on is that for *every* dessin D with valency lists V and C there exists a solution to the factorization problem (2.5) such that the corresponding Belyi function gives $D = \beta^{-1}([0, 1])$. This is a simplified version of the Grothendieck correspondence [7].

2.4. Action of the galois group

So far, we have mentioned repeatedly that the absolute Galois group $\Gamma = \mathrm{Gal}(\overline{\mathbb{Q}}/\mathbb{Q})$ acts faithfully on dessins. We now show how Γ acts on the dessins via the Belyi map.

Let D be a dessin such that $D = \beta^{-1}([0, 1])$. Furthermore, let β be of the form

$$\beta = \frac{A(z)}{B(z)} = \frac{z^{2N} + a_1 z^{2N-1} + \cdots + a_{2N}}{z^L + b_1 z^{L-1} + \cdots + b_L},$$

where $A(z)$ and $B(z)$ solve the polynomial equation (2.5), N is, as before, the degree of $P(z)$ and $L = \sum_{i=1}^{m} i v_i$. Then Γ acts on D by twisting the coefficients[6] in β. For $g \in \Gamma$, D_g is defined to be the dessin obtained by the

---

[6] The a_i (and b_j) are algebraic numbers; i.e., they are solutions to some polynomial equations with coefficients in $\mathbb{Q}$. The solutions to such equations include a_i along with other algebraic numbers which are, by definition, in the Galois orbit of a_i. Twisting by the relevant group element of Γ here refers to choosing another element in the orbit of a_i. For a more formal discussion, refer to Appendix A.

action of g on D, i.e., $D_g = \beta_g^{-1}([0,1])$, where

$$(2.9) \qquad \beta_g = \frac{A_g(z)}{B_g(z)} = \frac{z^{2N} + g(a_1)z^{2N-1} + \cdots + g(a_{2N})}{z^L + g(b_1)z^{L-1} + \cdots + g(b_L)}.$$

Thus, given a solution to the polynomial problem (2.5) it is easy to understand how the dessin changes under the action of the Galois group. However, given two dessins, it is in general very difficult to tell whether they belong to the same Galois orbit or not. This is the central problem associated to the dessins d'enfants. Later, we will discuss several Galois invariants that mathematicians have introduced in order to distinguish dessins that belong to distinct Galois orbits by studying the combinatorial data associated to each dessin.

2.5. The identification

We have already discussed the Seiberg–Witten curves for pure gauge theories in (1.1). Recall that for a $U(N)$ gauge theory with $L < 2N$ massive flavors with masses given by m_i, the Seiberg–Witten curve that captures the infrared dynamics of the gauge theory is the following hyperelliptic Riemann surface [17, 18]:

$$(2.10) \qquad y^2 = \langle \det(z\mathbb{I} - \Phi)\rangle^2 - 4\Lambda^{2N-L}\prod_{i=1}^{L}(z + m_i).$$

We would like to propose the following identification and argue that it is a useful one. Let us identify objects in (2.5) and in (2.10) as follows: $P_N(z) = \langle \det(z\mathbb{I} - \Phi)\rangle$, $B(z) = -4\Lambda^{2N-L}\prod_{i=1}^{L}(z - m_i)$. In particular, $\alpha = -4\Lambda^{2N-L}$. In each case, the precise form of $A(z)$ in (2.4) defines the special point in the Coulomb moduli space we are looking at. Since dessins are associated only to rigid factorizations of the Seiberg–Witten curves, they appear at isolated singular points in the moduli space of the $\mathcal{N} = 2$ gauge theory.

At this point, it appears as if the relation to Seiberg–Witten curves is purely at a formal level. We will show in what follows that this is more than a superficial similarity and we exhibit features of the gauge theory that have a natural interpretation as operations on the dessin. For this, we have to abandon our $\mathcal{N} = 2$ point of view and deform the theory to $\mathcal{N} = 1$ by a tree level superpotential as reviewed in Section 1.1.

We mentioned earlier that the absolute Galois group acts faithfully on the set of all trees. For most part of the paper, we will restrict our discussion to the set of trees and only in Section 6 will we discuss dessins with loops.

2.6. Trees on the Riemann sphere: refined valency lists

Since trees have only one open cell (with the associated vertex at infinity) the Seiberg–Witten curve associated to the dessin is that of the pure $U(N)$ gauge theory:

$$(2.11) \qquad y^2 = P_N^2(z) - 4\Lambda^{2N} .$$

By itself, the curve in (2.11) does not correspond to any dessin, but if we tune the parameters in $P_N(z)$ so that we are at an isolated singularity in the moduli space, the curve factorizes, and the zeroes of the polynomials involved will describe vertices of a dessin. This also means that the Belyi map (2.6) is a polynomial

$$(2.12) \qquad \beta(z) = \frac{A(z)}{B(z)} = 1 - \frac{P_N^2(z)}{4\Lambda^{2N}} ,$$

where $P_N(z)$ solves the factorization

$$(2.13) \qquad (P_N(z) - 2\Lambda^N)(P_N(z) + 2\Lambda^N) = \prod_{j=1}^{k}(J_{u_j}(z))^j .$$

From the expression it follows that the two factors on the left cannot have any factors in common. Thus, for trees, the problem always reduces to solving two lower order equations of the form

$$(2.14) \qquad \begin{aligned} P_N(z) - 2\Lambda^N &= \prod_{j=1}^{k}(Q_{u_j^-}(z))^j \\ P_N(z) + 2\Lambda^N &= \prod_{j=1}^{k}(R_{u_j^+}(z))^j \end{aligned}$$

such that $u_j^- + u_j^+ = u_j$ for every j. One can now define a new bipartite structure on the dessin by assigning a $+(-)$ to every zero of $R_{u_j^+}$ $(Q_{u_j^-})$ such that if a given vertex (pre-image of 0) is of one sign, every one of its neighbors is of the opposite sign. The bipartite structure is unique up to an overall sign flip. This leads to a more refined valency list $\{V^+, V^-\}$ than the $\{V, C\}$ introduced earlier[7] where $V_\pm$ denotes the positive/negative valency

---

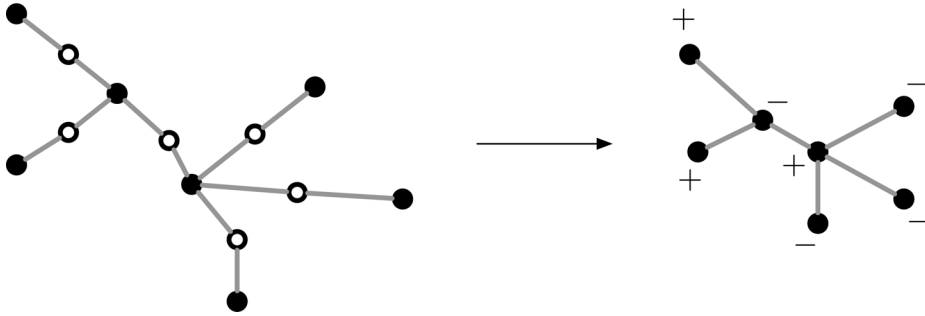[7] C contains just one element and is trivial for the case of trees.

Figure 8: Refined valency list for the trees. $V^+ = \{2, 0, 0, 1\}$ and $V^- = \{3, 0, 1\}$ for this case.

list. For instance, from (2.14) u_j^+ is the number of j-valent vertices of type "+". With the refined valency list, the trees can be redrawn as shown in the figure below.

Note that in the figure on the right, we have removed the pre-images of 1 depicted as ∘ on the left. This is common practice in the literature when dealing with trees. There is one more common convention which is to depict elements in V^+ by ● and elements in V^- by ∘; we have not adopted this convention in order to avoid confusion and we simply add $\pm$ to the ●'s as in figure 8.

Clearly, the dessins that arise from different valency lists belong to distinct Galois orbits; we will comment more about this in the next section.

Interestingly enough, there is a related splitting of the polynomial equation in the gauge theory. In [8], while solving the non-rigid problem (1.2), it was found that the $\mathcal{N} = 1$ branches are classified by the integers (s_+, s_-), where $s_\pm$ refers to the number of double roots in each of the factors on the left hand side of (2.14). This is already a hint that the mathematical goal of classifying dessins according to Galois orbits might be closely related to the more physical problem of studying the branches of $\mathcal{N} = 1$ vacua in gauge theory. We will see this in more detail in Section 4.

2.7. Equivalence classes of trees

Let us consider the Equations (2.14) in more detail. These equations have two free parameters corresponding to the scale and shift of z. In other words, if $P_N^{(1)}(z)$ is a solution then $P_N^{(2)}(z) = P_N^{(1)}(az+b)$ is also a solution. In physics as well as in mathematics, it is natural to consider monic polynomials. This means that a is restricted to be an Nth root of unity.

The trees constructed using the Belyi map (2.12) with $P_N^{(1)}(z)$ and $P_N^{(2)}(z)$ are identical except for a displacement or rotation in the z plane. In the mathematical literature, such trees are considered equivalent and one considers equivalence classes of such Belyi maps. The Grothendieck correspondence is in fact an isomorphism between equivalence classes of Belyi maps[8] and children's drawings.

Every tree has associated to it a number field (see Appendix A for a primer on field extensions) [15], determined by the field of definition of the polynomial $P_N(z)$ that gives the corresponding Belyi map (2.12). This might be a little puzzling at first, since the transformation $z \to az + b$ can in general involve arbitrary algebraic numbers. This means that the number field associated to trees that differ by translations and rotations can be different. On the other hand, we have just said that such trees are taken to define an equivalence class on which $\mathrm{Gal}(\overline{\mathbb{Q}}/\mathbb{Q})$ acts.

The resolution to this puzzle is that, although the Galois group acts nontrivially on all these trees, there is always a way of choosing the tree with the simplest number field [19] as a representative of the equivalence class. It turns out that the action of $\mathrm{Gal}(\overline{\mathbb{Q}}/\mathbb{Q})$ on just the representatives of each class is faithful. Therefore, for the purposes of studying the absolute Galois group one uses the shift and scale of z to pick the simplest representative.

All these statements have a counterpart in physics. The freedom to shift by b corresponds to the fact that the underlying theory is $U(N)$, as opposed to $SU(N)$. The overall $U(1)$ decouples in the IR and gives rise to this shift degree of freedom. Just like in mathematics, one can use this shift to bring any tree level superpotential to a form that displays the $\mathcal{N} = 1$ branches, introduced in Section 1, most clearly. We will use this in Section 5.

More intriguing is the meaning of the rescaling by an Nth root of unity. In physics, this corresponds to different kinds of confinement distinguished by the behavior of combinations of Wilson and 't Hooft loop operators. Roughly speaking, the trivial root of unity corresponds to usual confinement, whereas the other roots correspond to oblique confinement [8]. Quite nicely, the mathematical criterion of choosing the simplest number field corresponds in physics to choosing the phase with usual confinement.

It would be very interesting to explore the connection between the "not-so-simple number fields" and the oblique confining phases. However, since our goal is to establish a connection between dessins (in terms of equivalence

---

[8] The equivalence class of Belyi maps is, in fact, up to any $\mathrm{SL}(2,\mathbb{C})$ transformation. However, we have used one of these to put the pole at ∞. Thus, only shift and scale transformations remain.

classes) and gauge theory, we will restrict our study to physics phases with only usual confinement.

2.8. Example: the maximally confining $\mathcal{N} = 1$ vacua

For now, let us discuss as an example the simplest tree one can draw: a branchless linear tree with N edges. Such a tree has two vertices of valence 1 and $N - 1$ vertices of valence 2. From the general discussion above, it is easy to write down the corresponding Seiberg–Witten curve for this case:

$$(2.15) \qquad\qquad P_N^2(z) - 4 = (z^2 - 4)H_{N-1}^2(z).$$

Here we have set $\Lambda^N = 1$.

This Seiberg–Witten curve corresponds to points where $N - 1$ mutually local monopoles go massless. The $\mathcal{N} = 1$ vacua are obtained by perturbing the $\mathcal{N} = 2$ theory by a mass deformation, with $W_{\text{tree}} = \frac{1}{2}\text{Tr}\Phi^2$. The condition $\Lambda^N = 1$ has N different solutions that correspond to the N different maximally confining $\mathcal{N} = 1$ vacua[9]. However, as discussed above, we take the simplest solution, i.e., $\Lambda = 1$. The solution to this equation is well known and given in terms of Chebyshev polynomials[10]. In figure 9, the zeroes of $P_N(z)$ and $H_{N-1}(z)$ have been depicted showing how the branchless tree arises.
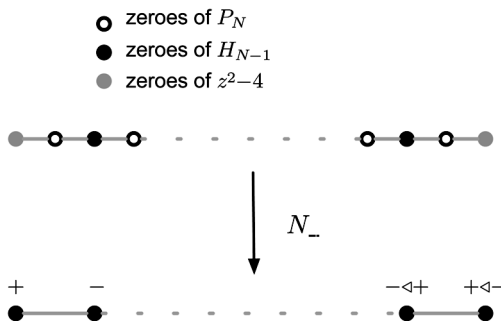

Figure 9: The dessin that corresponds to the maximally confining vacuum. Case by case, it is obtained by plotting the zeroes of the polynomials that solve the factorization problem (2.15). See for example figure 17 for the $N = 6$ plot.

---

[9] The reason for the name is that the low energy gauge group is just $U(1) \subset U(N)$.

[10] Here, the shift symmetry is used to set $\langle \text{Tr}\Phi \rangle = 0$.

The importance of the branchless tree lies in the fact that these appear at the intersection of the $\mathcal{N} = 1$ branches, the point marked by a cross in figure 1. They also appear near the semi-classical limits ($\Lambda \to 0$) as shown in figure 2. Although these truncated branchless trees cannot be thought of as dessins, they seem to be "building blocks" that come together to create a dessin at an isolated singularity. We discuss this point in more detail in the conclusions.

So far, we have been rather loose in the language employed to discuss aspects of the factorization problems. Techniques from both the physics and mathematics literature have been used interchangeably. We now turn to a more systematic discussion of how the dessins are classified from a mathematical point of view. We will follow this up with a review of how the $\mathcal{N} = 1$ vacua are classified from a physics point of view.

3. Invariants

3.1. Invariants from mathematics

One way of learning about the structure of the absolute Galois group $\mathrm{Gal}(\overline{\mathbb{Q}}/\mathbb{Q})$ is by constructing a complete set of invariants under the action of $\mathrm{Gal}(\overline{\mathbb{Q}}/\mathbb{Q})$ such that any two dessins that do not belong to the same Galois orbit will disagree in at least one invariant. Such a complete list of invariants is currently not known although many invariants have been constructed. In this section, we review the most basic invariants[11] associated to dessins that are related by the action of $\mathrm{Gal}(\overline{\mathbb{Q}}/\mathbb{Q})$ [15, 20].

3.1.1. Valency lists. The most intuitive invariants are the valency lists V and C introduced in Section 2. These are clearly invariants, since as we saw they are determined by the form of the polynomial equation which is invariant under the action of $\mathrm{Gal}(\overline{\mathbb{Q}}/\mathbb{Q})$. It is sometimes possible to define more refined valency lists, corresponding to different ways of solving the polynomial equation. We have already seen this for the case of trees, where we introduced the $\{V^+, V^-\}$ valency lists. As we discussed, this possibility of constructing a new invariant has a nice counterpart in physics; it will be further clarified in the examples that follow. Note that by concentrating on dessins coming from the same factorization problem we can forget about the valency list invariant since all dessins constructed this way have the same

---

[11] More invariants than those discussed here are known, but for the purpose of our analysis we will concentrate on those that can be most easily computed explicitly.

valence list. Therefore, the search is for other invariants that will distinguish different Galois orbits.

3.1.2. Monodromy group.   Every dessin is associated to a cover of $\mathbb{P}^1$, defined by the Belyi map

$$\beta : \Sigma \longrightarrow U \equiv \mathbb{P}^1 \backslash \{0, 1, \infty\} \,,$$

that maps the edges of the graph on the Riemann surface Σ into the open segment $\overline{01}$ on $\mathbb{P}^1$. If the graph has N edges, where we count the number of edges to be equal to the number of pre-images of 1, the map β gives a $2N$-fold cover of U (see figure 10 for an illustration).

Consider $\pi_1(U, \overline{01})$, the homotopy group of paths in U that begin and end on a point of $\overline{01}$. Since a closed path based on $\overline{01}$ in $\mathbb{P}^1$ can be mapped into a path between any two of the $2N$ segments in the fiber over $\overline{01}$, any given element of $\pi_1(U, \overline{01})$ acts on the dessin as a permutation of the half-edges (that go between a filled and unfilled vertex in figure 10). Therefore, the covering map β induces a map from $\pi_1(U, \overline{01})$ to S_{2N}. Let us denote by σ_0, the permutation corresponding to circling once the point $z = 0$ on $\mathbb{P}^1$ and by σ_1 the permutation corresponding to circling once the point $z = 1$. Recall that the dessins have a bipartite structure that keeps track of whether a vertex is mapped to 0 or 1 by the Belyi map. One can convince oneself that σ_0 is the element of S_{2N} that permutes cyclically the edges incident on each vertex (that maps to 0) and, similarly, σ_1 is a cyclic permutation of the edges incident on each pre-image of 1. The subgroup of S_{2N} generated by σ_0 and σ_1 is the monodromy group of the dessin and it is a Galois invariant [21].
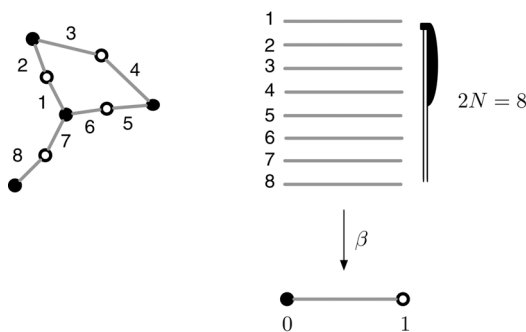

Figure 10: Left: Example of a dessin with $N = 4$ edges. Right: The 8 half-edges come from the preimage of the open interval $\overline{01}$, i.e. the preimage of 0 and 1 are not shown.

Let us consider the example of the dessin in figure 10. There are eight half-edges. The monodromy group is generated by the following permutations:

$$\sigma_0 = (1,7,6)(2,3)(4,5)\,,$$
$$\text{(3.1)}$$
$$\sigma_1 = (1,2)(3,4)(5,6)(7,8)\,.$$

We will give the explicit monodromy groups for the examples we will encounter later.

3.1.3. Belyi extending maps. It is possible to construct new invariants by composing the Belyi map of interest with any Belyi-extending map and then computing the valency lists or the monodromy group of the new dessins obtained this way [9]. A Belyi extending map is a Belyi map $\alpha : \mathbb{P}^1 \to \mathbb{P}^1$ defined over $\mathbb{Q}$, such that its composition with any other Belyi map does not change the associated number field. For our purposes, we relax the definition slightly: by a Belyi extending map here we will mean any map α defined over $\mathbb{Q}$ that can be composed with a Belyi map β to give another Belyi map $\beta_\alpha := \alpha \circ \beta$.

Let I be any invariant of a dessin D_α, where $D_\alpha = \beta_\alpha^{-1}([0,1])$; the claim [9] is that I is also an invariant of the dessin $D = \beta^{-1}([0,1])$. For example, for the Belyi extending map $\alpha_2(z) = 4z(1-z)$, the monodromy group of D_α is the cartographic group of D, which is known to be another Galois invariant. Later we will prove that the multiplication map of [10, 8] is the physical realization of the Belyi extending map α_2.

3.2. Invariants from physics

As discussed in Section 1, one problem that is very similar to the classification of dessins using Galois invariants is the problem of classifying branches of $\mathcal{N} = 1$ vacua using order parameters, such as Wilson and 't Hooft loops. We will consider those $\mathcal{N} = 1$ vacua that are obtained in the infrared by starting with an $\mathcal{N} = 2$ gauge theory and adding a tree level superpotential W_{tree} for the adjoint scalar Φ. The discussion of the gauge theory order parameters in this section will closely follow that of [8]. In fact, what follows is just a summary. We refer the reader to [8] for all relevant details and proofs.

3.2.1. Confinement index. In a $U(N)$ gauge theory a natural order parameter is the expectation value of a Wilson loop W in, say, the fundamental representation. The Wilson loop in the tensor product of r fundamental

representations is W^r. Clearly, for $r = N$ there is no area law, for it is equivalent to a singlet representation (due to electric screening). A measure of confinement is the smallest value of r, which can only be between 1 and N, for which W^r does not exhibit an area law. Such a value is denoted by t and it is called the confinement index. When the gauge group is broken classically to a product of factors $U(N_1) \times U(N_2) \times \cdots \times U(N_n)$ one has to also use the 't Hooft loop H to determine the confinement index. By embedding a 't Hooft–Polyakov magnetic monopole of the full $U(N)$ theory in any two of the $U(N_i)$ factors, we take into account magnetic screening. If for each $U(N_i)$, we get that $W_i^{r_i} H_i$ has no area law, this implies that in the full $U(N)$ theory $W^{r_i - r_j}$ has no area law. The relative sign comes from the fact that the magnetic monopole sits in both groups with opposite charges.

Therefore, after taking into account electric and magnetic screening, the confinement index is given by the greatest common divisor of the N_i and $b_i = r_i - r_{i+1}$. These two sets of quantities, N_i's and b_i's, will have a very clear combinatorial meaning, which will allow us to compute the confinement index just by inspection of any dessin.

As a preparation for that let us mention that both set of quantities are encoded in the expectation values of the generating function for chiral operators $\mathrm{Tr}\Phi^s$, given by [22]

$$(3.2) \qquad T(z) = \left\langle \mathrm{Tr} \left(\frac{1}{z\mathbb{I} - \Phi} \right) \right\rangle .$$

It turns out that the periods of $T(z)dz$, thought of as a meromorphic differential on $y^2 = W'_{\mathrm{tree}}(z)^2 + f_{n-1}(z)$, are related to the N_i's and b_i's as follows: the N_i's are the periods of $T(z)dz$ on the A-cycles and the b_i's are the periods of $T(z)dz$ on the B-cycles (for an appropriate choice of basis). The b_i's measure the relative theta angle of $U(N_i)$ and $U(N_{i+1})$. Moreover, one can show that in the $\mathcal{N} = 1$ branch with confinement index t, $T(z)\,dz = t\widetilde{T}(z)\,dz$, where $\widetilde{T}(z)\,dz$ is the generating function for chiral operators in a Coulomb vacuum (which have $t = 1$) of a $U(\frac{N}{t})$ theory [8]. The fact that the two generating functions are related by a multiplication by t has an important consequence: all confining vacua with confinement index t are obtained from Coulomb vacua by using the multiplication map by t [10, 8]. The definition and discussion of the multiplication map is given in Appendix B. We also discuss this further in Section 4.1 where, for the specific case of $t = 2$, the multiplication map will be shown to coincide with the Belyi extending map α_2 of [15].

3.2.2. Holomorphic invariants. In cases when the rank of the low energy gauge group is too high, i.e., when the degree of the tree level superpotential is large, there is always at least one N_i which is equal to 1. The precise condition is $\deg W'(z) > N/2$: when this condition is satisfied, the confinement index is always one. One might naively think that there is only one branch since we have exhausted the standard order parameters. However, it is possible to show that there are many branches, all of them having Coulomb vacua. This is the problem that motivated the search for nonconventional order parameters in [8]. It turns out that the discussion that follows also applies for superpotentials of any degree.

The new non-conventional order parameters proposed in [8] are obtained by studying relations between the vacuum expectation values of different chiral operators that can be defined in the theory. The expectation values of chiral operators become holomophic functions on the moduli space of vacua due to supersymmetry. It turns out that, at least in the examples considered in [8], these functions satisfy different polynomial constraints in different branches. The problem of whether the existence of these relations was the reason for the existence of the different branches or viceversa was left as an open question. For the purposes of this paper, we take the former as the correct point of view. In fact, we will see that in the mathematical literature the refined valency list for trees gives very similar information as the relations between holomorphic functions found in [8].

The chiral operators of relevance are $\mathrm{Tr}\Phi^r W_\alpha W^\alpha$, whose appropriately normalized vacuum expectation value is denoted by $t_r = -(1/32\pi^2)\langle\mathrm{Tr}\Phi^r W_\alpha W^\alpha\rangle$. In terms of the reduced Seiberg–Witten curve $y^2 = F_{2n}(z)$, they can be computed as[12]

$$(3.3) \qquad t_r = \frac{1}{2\pi i} \oint_\infty z^r \, y(z) \, dz \, .$$

The relations introduced in [8] to distinguish between different branches are polynomial equations in the t_r's.

The different branches that these relations distinguish are determined by the distribution of double zeroes of the curve (2.6) in the two factors of $P_N^2(z) - 4\Lambda^{2N}$, i.e., by the pair (s_+, s_-). In other words, if we start with the

---

[12] Strictly speaking, the curve needed for the computation is given by the matrix model curve of the Dijkgraaf–Vafa correspondence. However, in cases when none of the N_i are zero, the matrix model curve is the same as the reduced Seiberg–Witten curve.

factorization problem $P_N^2(z) - 4\Lambda^{2N} = F(z)H^2(z)$, we get

(3.4)
$$P_N(z) - 2\Lambda^N = \widetilde{R}_{N-2s_-}(z)\widetilde{H}_{s_-}^2(z),$$
$$P_N(z) + 2\Lambda^N = R_{N-2s_+}(z)H_{s_+}^2(z).$$

In order to derive the relations it is convenient to write
(3.5)
$$y(z) = \sqrt{\widetilde{R}_{N-2s_-}(z)R_{N-2s_+}(z)} = \frac{H_{s_+}(z)R_{N-2s_+}(z)}{\widetilde{H}_{s_-}(z)}\sqrt{1 - \frac{4\Lambda^N}{H_{s_+}^2(z)R_{N-2s_+}(z)}}.$$

Since the integral defining the t_r's is around infinity, the computation can be carried out by expanding the square root. It is easy to see that if $0 \le r \le s_+ + s_- - 2$ then only the leading term in the expansion contributes. It turns out that in order to distinguish different values of (s_+, s_-) all that is needed are relations between those (restricted) t_r's. Using the fact that Λ does not appear, by matching dimensions (which for t_r is $3 + r$) and by matching the charge under the $U(1)_\Phi$ symmetry (which for t_r is r), one concludes that the polynomials must be homogeneous in the number of Φ's and the number of $W_\alpha W^\alpha$. Consider for example, the case when $s_- = 1$ and $s_+ = 3$. Then one can show that $t_0 t_2 - t_1^2 = 0$.

We will see in the next section that (s_+, s_-) gives some information about the refined valency list of a dessin. However, the refined valency list contains more information. In Section 5.2, we will show by means of examples that the extra information of the refined valency list can be obtained if one keeps the next to leading order term in the expansion of the square root. In other words, in the expansion

(3.6)
$$\sqrt{1 - \frac{4\Lambda^N}{H_{s_+}^2(z)R_{N-2s_+}(z)}} = 1 - \frac{2\Lambda^N}{H_{s_+}^2(z)R_{N-2s_+}(z)} + \mathcal{O}(\Lambda^{2N}/z^{2N}),$$

the first term gives information about (s_+, s_-), whereas the second encodes the whole refined valency list. It would be interesting to find a combinatorial meaning of the higher order terms. It is important to mention that the extra relations we find distinguish the isolated point where the dessin appears from its neighbouring points in the $\mathcal{N} = 1$ branch.

4. Cross fertilization

Before we discuss some examples to illustrate our ideas, we would like to exhibit part of the dictionary between the mathematical and physical descriptions. First, we show how the multiplication map [10] can be interpreted as an example of a Belyi extending map [20]; we also show that the information about the refined valency list of trees, described in Section 2.7, can be recovered by studying the holomorphic invariants. Most importantly, we give a combinatorial interpretation of the confinement index introduced in [8]. We then speculate on the relation between the classification of dessins and the study of phases of gauge theories in four dimensions and formulate a few precise conjectures.

4.1. Multiplication map as a Belyi extending map

Consider a tree with N edges. The Belyi map has the form (2.12)

$$\beta_N(z) = 1 - \frac{P_N^2(z)}{4\Lambda^{2N}}\,.$$

The dessin corresponds to a rigid polynomial equation, which is a special point in the parameter space of the non-rigid factorization problem

(4.1)
$$P_N^2(z) - 4\Lambda^{2N} = F_{2n}(z)\,H_{N-n}^2(z)\,.$$

The multiplication map [10] (with multiplication factor 2) guarantees that, if $P_N(z)$ satisfies the non-rigid factorization equation (4.1), one solution to the factorization equation

$$P_{2N}^2(z) - 4\Lambda^{4N} = F_{2n}(z)\,\widetilde{H}_{2N-n}^2(z)$$

is given by (see Appendix B for details)

(4.2)
$$P_{2N}(z) = 2\Lambda^{2N}\,T_2\left(\frac{P_N(z)}{2\Lambda^N}\right),$$

where $T_2(x) = 2x^2 - 1$ is a Chebyshev polynomial of the first kind. Since $P_N(z)$ gives rise to a Belyi map, $P_{2N}(z)$ as defined in (4.2) also leads to a Belyi map β_{2N} whose inverse image of the interval $[0,1]$ leads to a dessin with $2N$ edges. Therefore, by applying the multiplication map, we get a new

Belyi map of the form

$$\beta_{2N} = 1 - \frac{P_{2N}^2(z)}{4\Lambda^{4N}} = 1 - \left(2\,\frac{P_N^2(z)}{4\Lambda^{2N}} - 1 \right)^2$$

(4.3)

$$= \frac{P_N^2(z)}{\Lambda^{2N}} \left(1 - \frac{P_N^2(z)}{4\Lambda^{2N}} \right) = 4\,\beta_N(1 - \beta_N)$$

$$\equiv \alpha_2 \circ \beta_N \,,$$

with $\alpha_2(y) = 4y(1-y)$. We thus find that this map coincides with the Belyi extending map mentioned in Section 3.1, which relates the monodromy group to the cartographical group.

In [20] the author gives a prescription to draw the dessin associated with any Belyi extending map starting from the original dessin. Roughly, the procedure consists in drawing on $\mathbb{P}^1$ the pre-image through the Belyi extending map of the $[0,1]$ segment; then, one substitutes this new drawing in place of each segment of the original dessin. Let us apply this to our example. The map α_2 is of degree two, so it covers $[0,1]$ twice and we expect it to double the number of edges of the dessin. More precisely, the critical point $y = 1/2$ is mapped by α_2 to the vertex $z = 1$ of the $[0,1]$ segment. Therefore, we infer the following rule to draw the dessin obtained through the Belyi extending map α_2:
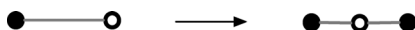
One could check that for generic t the multiplication map by t is a Belyi extending map that substitutes to each edge in the original graph a branchless tree of length t. Naively, the dessins with confinement index 2 or higher would appear to be "scaled up" versions of smaller dessins. Indeed, this is what one gets if one applies the multiplication map to the rigid factorizations that lead to the dessins.

However, from the gauge theory point of view, one can also apply the multiplication map to the non-rigid problem (4.1) and *then* impose the constraints that leads to a rigid factorization problem. In other words, if $\mathcal{F}_{R/NR}$ is the set of rigid/non-rigid factorizations and if M is the multiplication map acting on the factorizations $\mathcal{F}$,

(4.4) $$M(\mathcal{F}_R) \subset (M(\mathcal{F}_{NR}))_R \,,$$

where the last subscript R indicates that the factorizations are restricted to be rigid. This shows that the multiplication map is more than an operation

to get new Belyi maps from old ones. Starting from a point in the moduli space of a $U(N)$ gauge theory which is *not* an isolated singularity (so that there is no associated dessin), one can apply the multiplication map by t and sometimes obtain a singular point in the moduli space of the $U(tN)$ theory where one *can* obtain a dessin. We will discuss such examples in Section 5. Moreoever, we will also see in Section 4.3, that applying the multiplication map to non-rigid factorizations is what allows us to prove that the confinement index is a Galois invariant.

4.2. Refined valency lists from (refined) holomorphic invariants

We have already mentioned in Section 2.7 that while solving the non-rigid problem (1.2) it is convenient to classify the solutions in terms of integers (s_+, s_-), where $s_\pm$ refers to the number of double roots in either of the two factors $(P(z) \pm 2\Lambda^N)$. We would now like to relate these numbers to the refined valency list introduced in Section 2.7. From the definitions one can check that a given dessin with refined valency lists $V^+ = \{u_k^+\}$ and $V^- = \{u_k^-\}$ will appear in an $\mathcal{N} = 1$ branch whose (s_+, s_-) values are given by[13]

$$(4.5) \qquad\qquad s_\pm = \sum_{k=1}^{\infty} k\, u_{2k}^\pm\,.$$

Recall that u_k is the number of k-valent vertices in the dessin. Clearly, the refined valency list contains more information than just the values of $s_\pm$.

From the discussion in Section 3.2, we have seen that the set of relations between the expectation values of chiral operators t_r's depends upon the distribution of double roots $s_\pm$, i.e., different branches are defined by the different polynomial relations between the t_r's. These chiral ring relations are satisfied at any generic point on that branch. However, the dessins appear only at special points in that moduli space. A simple counting of parameters shows that at such points there will be more relations that are not generically satisfied. We will, in the examples to be discussed in Section 5, write down these extra relations satisfied by the t_r's explicitly.

---

[13] In assigning a refined valency list to a dessin, there is an overall choice of sign in assigning $+/-$ to the vertices. It follows that this amounts to exchanging s_+ and s_-. The same choice is also present in gauge theory.

Since the generic relations seem to distinguish branches of $\mathcal{N} = 1$ vacua, it is tempting to conjecture that these special points are isolated phases. In other words, they are distinct phases from their neighbours in the $\mathcal{N} = 1$ branch. That this is the case is easy to see in some cases where the corresponding $\mathcal{N} = 1$ theory becomes superconformal in the IR. Moreover, it is believed that there is always a choice of superpotential for which the resulting $\mathcal{N} = 1$ vacuum flows to an interacting superconformal theory [8, 23, 24].

4.3. Confinement index as a Galois invariant

The physical interpretation of the confinement index t was given earlier in this section. We also explained how t can be computed from the periods of a particular meromorphic differential $T(z)dz$ on the Seiberg–Witten curve. Here, we first give a purely combinatorial description of the confinement index t. Then, we show that this is indeed a Galois invariant.

Consider a given tree T, constructed as T= $\beta^{-1}([0, 1])$ under a clean Belyi map $\beta(z) = 1 - P(z)^2$, where $P(z)$ is a polynomial. Let us concentrate on the pre-images of 0 under β. There can be vertices with any valency. In particular, there must be vertices with valence one; this is a simple consequence of the fact that the Belyi map is clean.

The procedure for computing t is the following: circle all vertices with odd valence. Choose any of the circled univalent vertices as the starting point. Move from the chosen vertex to the next circled vertex, say going clockwise around the tree, and count the number of edges between the two circled vertices; call it h_1. Move from the second circled vertex to the next circled vertex. Again count the number of edges between the two vertices; call it h_2. The most important rule to apply when going around the tree is that each circled vertex can be used only once as a starting point and only once as an end point. Therefore, if the next vertex was used previously both as an end point and as a starting point, one should skip it and go to the next one. Continue around the tree until there are no more unused circled vertices. The prescription makes sense because there is an even number of odd-valent vertices[14].

After completing this procedure, one is left with a list of integers $\mathcal{L} = \{h_1, h_2, \ldots, h_f\}$, where f is the number of odd vertices in the dessin. Then t is simply given by the greatest common divisor of the elements of $\mathcal{L}$. Two

---

[14] That there is an even number of odd vertices is clear from the fact that β is a polynomial of even degree.

simple examples are shown below.
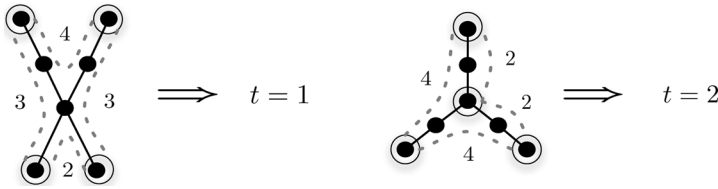
This rule works because the vertices with odd valence are precisely the points between which one would draw the cuts in the gauge theory approach. Then, this definition can be seen to coincide with the definition of the confinement index introduced in [8]. This follows from the fact that the integral of $T(z)\,dz$ between successive vertices is 1.

Having given a purely combinatorial definition of t we proceed to show that this is indeed a Galois invariant. The proof involves concepts and terminology reviewed in Appendix A.

Let us consider all possible trees with a fixed number of edges N. If N is prime then the only possible values of t are $t = 1$ and $t = N$. The only tree with $t = N$ is the branchless tree which is a tree defined over $\mathbb{Q}$ and hence it is its own Galois orbit[15]. All other trees have $t = 1$, so there is nothing further to prove.

Consider an N which is not prime. Let $N = p_1^{r_1} \cdots p_s^{r_s}$ be the prime decomposition of N. Take any p_i and consider the auxiliary polynomial $P_{p_i}(z)$. Use the multiplication map by $m = N/p_i$ to produce what we called a non-rigid curve (for more details on the multiplication map see Appendix B)

$$(4.6) \qquad 1 - T_m^2(P_{p_i}(z)) = (1 - P_{p_i}^2(z))U_{m-1}^2(P_{p_i}^2(z)).$$

This depends on the $p_i + 1$ coefficients of $P_{p_i}(z)$. As discussed in Section 2.2, the new $\widetilde{P}_N(z) = T_m(P_{p_i}(z))$ gives rise to a Belyi map $\beta(z) = 1 - \widetilde{P}_N^2(z)$ if and only if $\widetilde{P}_N'(z)$ divides the right hand side of (4.6). This is equivalent to imposing that the right hand side of (4.6) has only $N - 1$ distinct roots. These conditions will give rise to polynomial equations for the coefficients of $P_{p_i}(z) = a_0 z^{p_i} + \cdots + a_{p_i+1}$. Let the set of polynomials that must vanish be $\mathcal{S} = \{f_1(a), \ldots, f_j(a)\}$. Since all Chebyshev polynomials $T_m(z), U_{m-1}(z)$ have coefficients in $\mathbb{Q}$ it follows that $f(a) \in \mathbb{Q}[a_0, \ldots, a_{p_i+1}]$. Therefore, there is a splitting number field $K_{\mathcal{S}}$ associated to the set $\mathcal{S}$. It is

---

[15] Here, what we have in mind is the branchless tree with the simplest number field, which in this case it is $\mathbb{Q}$.

a finite normal extension of $\mathbb{Q}$ and hence is left invariant by $\text{Gal}(\overline{\mathbb{Q}}/\mathbb{Q})$. This means that the solutions form full Galois orbits. From the relation between the multiplication map and the confinement index t it follows that all such orbits can only have values of t which are multiples of m that divide N. This means that either $t = m = N/p_i$ or $t = p_i m = N$. As mentioned above, there is a single tree with $t = N$ and therefore all other orbits must have the same value $t = N/p_i$.

Consider now $k = p_i p_j$ and the polynomial $P_k(z)$. As before, use the multiplication map by $m = N/k$. Following the same procedure, we conclude that dessins arising this way can only have values of t which are multiples of m and that divide N. The only possibilities are $t = N/k, N/p_i, N/p_j, N$. As before, $t = N$ gives a single tree. We have already proven that dessins with $t = N/p_i$ or $t = N/p_j$ can only come in full Galois orbits. Therefore, the remaining dessins with $t = N/k$ also arise in full Galois orbits.

One can continue this argument by induction and conclude that any two dessins in the same Galois orbit must have the same confinement index t. Thus, the confinement index is a Galois invariant.

4.4. Speculations about dessins and gauge theory: weak and strong conjectures

We now have all the ingredients we need to formulate our conjectures precisely. We have already seen that there exist $\mathcal{N} = 1$ branches in pure gauge theory that are classified by order parameters such as the confinement index. Also, as mentioned in Section 4.2 (and as we will show in some simple examples), at the special points where the dessins appear one has extra chiral ring relations. For an appropriately chosen superpotential, these points are believed to give rise to superconformal $\mathcal{N} = 1$ theories in the IR and thus define new phases. However, it is known that for some superpotentials, these theories might not be singular. This does not exclude the possibility that these points might be new phases, perhaps distinguished by less exotic behavior, such as extra massless states or smaller rank of the gauge group.

Given the earlier discussion regarding the theory of dessins and the phases of supersymmetric gauge theory, our first conjecture should be fairly well motivated: all points where dessins appear correspond to special phases embedded in the $\mathcal{N} = 1$ branches which we call "isolated phases".

Our second conjecture, relating the phases to Galois orbits of dessins has a weak and a strong form. The strong form is easily stated: all Galois invariants are physical order parameters that can be used to distinguish the isolated phases of supersymmetric gauge theory with a given superpotential.

On the other hand, based on the examples we work out in Section 5, we find that all the order parameters used to distinguish branches of gauge theories that meet a particular $U(1)$ branch, defined below, are Galois invariants. This is what we refer to as the weak form of the conjecture.

Some comments are in order. By a $U(1)$ branch, we mean a branch where the low energy group is a single $U(1) \subset U(N)$. This can be called the maximally confining branch. This branch has the same dimension as the other branches [8]. Any generic branch meets these $U(1)$ branches at points where the corresponding dessin is a branchless tree with N edges.

We believe that the weak form of the second conjecture is very likely to be correct and we provide evidence for it in the examples. The strong form is on much less firm ground. In particular, it relies on the correctness of the first conjecture and on assumptions that require much more study.

It would be very important to gather more evidence for the strong form since, if true, it provides a striking connection between Grothendieck's program of unveiling the structure of $\text{Gal}(\overline{\mathbb{Q}}/\mathbb{Q})$ via its action on dessins and the physics problem of classifying phases of supersymmetric gauge theories. Some of the most striking consequences would be for gauge theories with matter where physics order parameters are scarce. Almost all known Galois invariants would become new gauge theory order parameters. In the next sections, we will provide some evidence in support of these conjectures.

4.4.1. A more general $\mathcal{N} = 1$ viewpoint and a global $\mathcal{N} = 2$ viewpoint.

The possibility that there is always an "extremal" superpotential for which the $\mathcal{N} = 1$ $U(N)$ gauge theory at one of the isolated singular points becomes superconformal in the IR motivates the following point of view. Up to now, we have studied theories with a superpotential of a given degree. However, if we fix $U(N)$ and vary the degree of the superpotential, the theories arising at the points where a dessin D appears can go from being non-singular to singular in the IR. Let us denote by $d(D)$, the smallest degree of an extremal superpotential for D. It is tempting to conjecture that two theories that arise at points corresponding to two dessins D and D' in the same Galois orbit will necessarily have $d(D) = d(D')$. In other words, $d(D)$ might be a Galois invariant. We leave this problem as an interesting direction for future work.

Finally, let us comment on yet another point of view. Suppose that we set the tree level superpotential to zero. Then we recover an $\mathcal{N} = 2$ gauge theory. The Seiberg–Witten curve of Section 2.5 becomes the curve describing the physics in the moduli space of vacua of a single theory. The valency lists C and V of Section 2.3 simply encode information about the masses of particles

in the theory. More explicitly, C determines the distribution of masses of fundamental hypermultiplets. V determines, up to modular transformations, the charges of the various monopoles and dyons that are massless in addition to the $U(1)^N$ vector multiplets present at generic points. According to the cases studied in the literature, there is reasonable evidence to suspect that all such points are $\mathcal{N} = 2$ superconformal field theories[16].

It would be very interesting to explore the relation between the classification of dessins into Galois orbits and the classification of such $\mathcal{N} = 2$ superconformal field theories. A natural possibility, worth exploring, is that field theories giving rise to dessins in the same Galois orbit might be dual theories in some sense.

5. Examples: $U(6)$ pure gauge theory

In this section, we would like to illustrate by means of examples the concepts we have covered up to now. We consider pure $\mathcal{N} = 2\, U(6)$ gauge theory broken to $\mathcal{N} = 1$ by a tree level superpotential. From the general discussion about dessins and polynomial equations, it follows that the $\mathcal{N} = 2$ moduli space contains an isolated singularity for every connected tree with six edges. It turns out that *all* such dessins can be obtained by just using a quartic superpotential. We discuss why higher degree superpotentials are not needed and list all dessins with their corresponding factorization problems in Appendix C.

Here, we restrict our study to a cubic superpotential. The dessins we obtain are, of course, a subset of the general quartic superpotential but they turn out to exhibit all the relevant points of the physics–mathematics dictionary we have established. All $U(N)$ gauge theories with $N = 2, \ldots, 6$ were studied in detail in [8] where one parameter solutions to the factorization problem

$$(5.1) \qquad\qquad P_N(z)^2 - 4\Lambda^{2N} = F_4(z)\, H_{N-2}^2(z)$$

are listed. In fact, the analysis in this section can be easily repeated for all these cases. We choose $U(6)$ because it is the simplest case that exhibits four different values of the confinement index, i.e., $t = 1, 2, 3, 6$.

---

[16] Of course, the point with $N - 1$ mutually local massless monopoles is not a superconformal field theory. In this case one can write down, using S-duality, a local lagrangian describing the full behavior of the theory in the IR.

The rigid factorizations corresponding to dessins are obtained by imposing suitable conditions on the solutions found in [8] along the lines we described in Section 1. In Sections 5.1 and 5.2, we classify the dessins according to the $\mathcal{N} = 1$ branches to which they belong and specify the order parameters that distinguish the special points where the dessins appear as isolated phases.

From a mathematical point of view, in order to find the explicit Belyi maps, it is not necessary to start from the non-rigid problem (5.1). Instead, one solves the rigid problems directly. In Section 5.3, we will present the solution to all possible rigid factorization problems that can be derived from (5.1) along the lines of [16] by using differentiation tricks. This analysis shows explicitly the classification of trees into distinct Galois orbits. In Section 5.4, we will reproduce the same classification of dessins using some of the known Galois invariants. We will find that this parallels the classification of phases in gauge theory.

We mentioned in Section 2.7 that, both in the physics and mathematical analysis, there is the freedom to shift and scale the z variable. From a physics perspective, it is natural [8] to shift the z variable in order to bring the superpotential to the canonical form $W'_{\text{tree}}(z) = z^2 - \Delta$ and then analyze the $\mathcal{N} = 1$ branches obtained by varying Δ. However, since our primary goal is to exhibit the dessins and where they appear in the gauge theory moduli space, in the examples that follow, we have followed the mathematical strategy to shift and scale z to put the solution in the simplest form possible, so that the number field associated to the tree is the simplest.

5.1. $U(6)$ gauge theory: a physicist's point of view

Let us now review the solution of [8] in detail. We then specialize to rigid factorizations by tuning the one free parameter available in the solutions to (5.1).

As described in [8] one can, first of all, classify $\mathcal{N} = 1$ branches by the number of double roots in either factor $(P_6(z) \pm 2\Lambda^6)$. If we denote the number of double roots in either factor as (s_+, s_-), in our case, these can take the values $(3, 1)$, $(1, 3)$ and $(2, 2)$. All these branches meet at vacua that have $(s_+, s_-) = (3, 2)$ or $(2, 3)$ at which the branchless tree discussed in Section 2.7 appears. The $\mathcal{N} = 1$ branches are further classified by the confinement index and the non-conventional order parameters which we defined earlier in Section 3.2. Let us consider each value of (s_+, s_-) in turn.

5.1.1. The (3, 1) and (1, 3) confining vacua. The general factorization problem (5.1) is solved by the polynomials[17]

(5.2)
$$P_6(z) + 2\eta\Lambda^6 = ((z-a)^2(z-b) - 2\epsilon\Lambda^3)^2 \equiv R^2(z)$$
$$P_6(z) - 2\eta\Lambda^6 = (z-a)^2(z-b)((z-a)^2(z-b) - 4\epsilon\Lambda^3) \equiv S(z)$$

with $\eta^2 = 1$ and $\epsilon^2 = \eta$. These polynomials can by obtained by the "multiplication by 2" map acting on either of the polynomials $P_3(z) = (z-a)^2(z-b) \mp 2\Lambda_0^3$:

(5.3)
$$P_6(z) = 2\Lambda^6\kappa^2\, T_2\left(\frac{P_3(z)}{2\kappa\Lambda^3}\right),$$

with $\Lambda_0^6 = \kappa^2\Lambda^6$, $\kappa^4 = 1$ and $\epsilon = \pm\kappa$. The various signs and phases in these expressions are crucial so that all the $\mathcal{N} = 1$ vacua are taken into account. However, as discussed in Section 2.7, since these lead to trees in the same equivalence class, we will drop such phase factors in what follows.

5.1.1.1. The rigid quartic factorization. If we require that the polynomial $R(z)$ has a double root (which is to say that its discriminant vanishes) we get the rigid factorization

(5.4)
$$P_6(z)^2 - 4\Lambda^{12} = F_4(z)\, H_2^2(z)\, Q_1^4(z).$$

This fixes Λ to be

(5.5)
$$\Lambda^3 = \frac{2}{27}(a-b)^3.$$

Substituting this into the polynomials in (5.2) and using the shift and scaling symmetry to set $a = -5$ and $b = 10$, we get

(5.6)
$$R^2(z) = (z-5)^4(z+10)^2,$$
$$S(z) = (z+5)^2(z-10)(z^3 - 75z + 750).$$

From this, we see that the polynomials that solve the equation

(5.7)
$$P_6^2(z) - 4(250)^4 = F_4(z)\, H_2^2(z)\, Q_1^4(z)$$

---

[17] Refer to Equation (3.47) in [8].

are given by
(5.8)
$$Q_1(z) = z - 5, \quad H_2(z) = (z + 5)(z + 10), \quad F_4 = (z - 10)(z^3 - 75z + 750),$$
$$P_6(z) = z^6 - 150z^4 + 500z^3 + 5625z^2 - 37,500z - 62,500.$$

Plotting the zeroes of the polynomials leads to the tree in figure 11. Let us make a few comments about the solution. All polynomials are defined over $\mathbb{Q}$. From the discussion in Section 2.4 about the action of the Galois group, we see that the tree is left invariant; in other words, it is the only element in its Galois orbit. From (5.3) we see that the tree has confinement index 2. However, observe that the tree is *not* a scaled up version of a smaller tree. This illustrates the point made in Section 4.1 and especially Equation (4.4). One can moreover check that the combinatorial method for computing the confinement index, as explained in Section 4.2, also gives the correct answer $t = 2$.

5.1.1.2. The rigid cubic factorization.   Starting from (5.1) one can also get another rigid factorization by tuning one of the zeroes of $F_4(z)$ to coincide with a zero of $H_4(z)$:

(5.9) $$P_6^2(z) - 4\Lambda^{12} = F_3(z)\, H_3^2(z)\, Q_1^3(z).$$

This leads to the condition $a = b$ in (5.2). This implies that $S(z)$ has a cubic root at $z = a$. Using the shift and scale symmetry, we can set $a = 0$ and
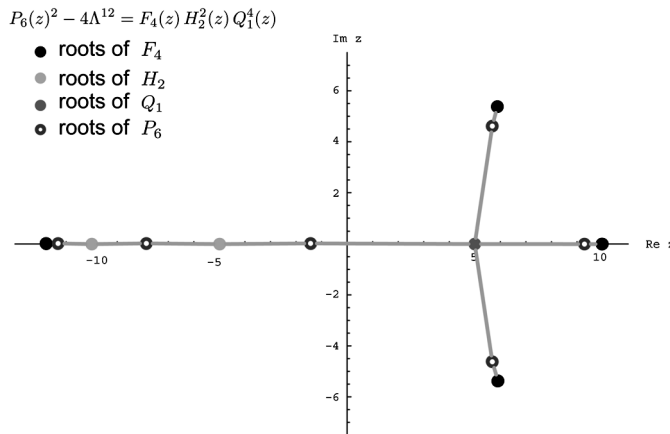

Figure 11: The tree obtained in the $(3, 1)$ confining branch with a four-valent vertex. It has confinement index $t = 2$.

$\Lambda = 1$. This leads to a very simple solution of (5.9) :

$$P_6(z) = z^6 - 4z^3 + 2, \quad H_3(z) = z^3 - 2, \quad F_3(z) = z^3 - 4 \quad \text{and} \quad Q_1(z) = z.$$

The tree associated to the factorization is drawn below in figure 12.

Note that, unlike the quartic case, the multiplication by 2 is easily under-stood: this particular solution can also be obtained by first solving the rigid
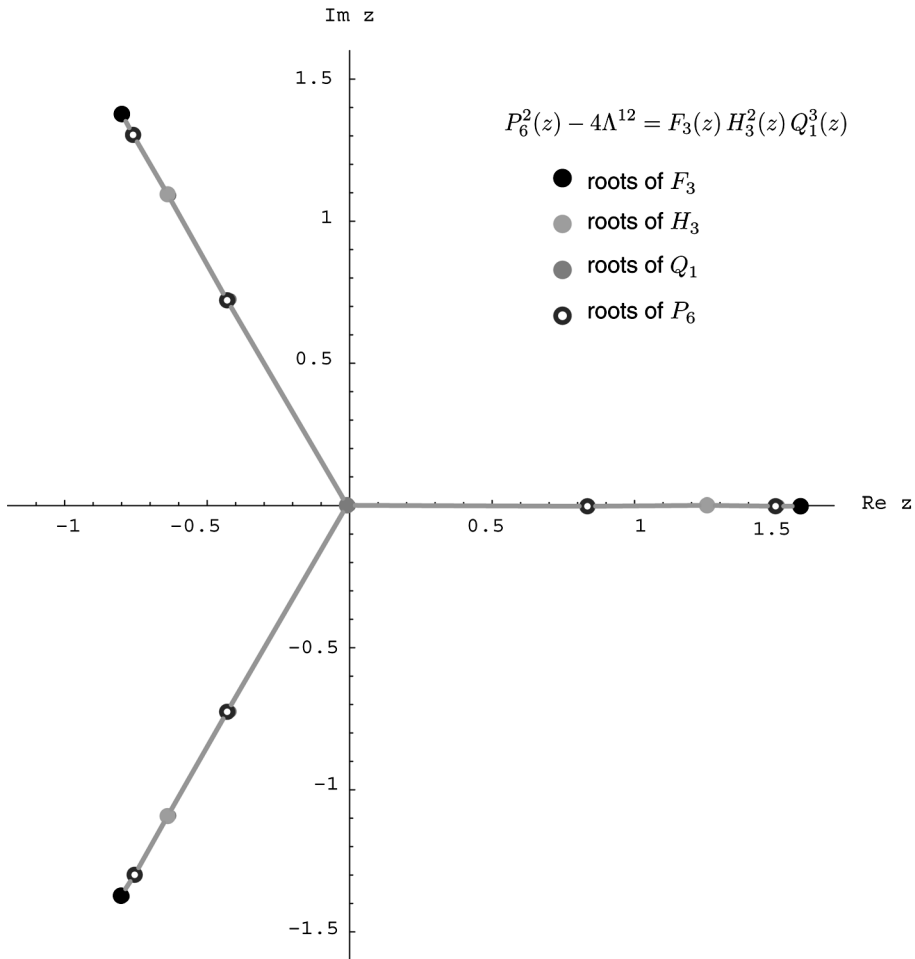

Figure 12: Tree obtained in the $(3, 1)$ confining branch with a trivalent vertex. It is a scaled up dessin, obtained by applying the multiplication map on a smaller dessin with three edges.

factorization problem

$$(5.10) \qquad\qquad P_3^2(z) - 4\Lambda^6 = Q_1^3(z)\, F_3(z)\,,$$

and then applying to the resulting solution the multiplication map. The solution is once again defined over $\mathbb{Q}$ and the tree in figure 12 is the lone element in its Galois orbit.

5.1.2. The $(2, 2)$ confining vacua.   In this sector, the factorization problem (5.4) is solved by the polynomials[18]

$$(5.11) \qquad \begin{aligned} P_6(z) + 2\Lambda^6 &= (z^2 + g - \Lambda^2)^2(z^2 + g + 2\Lambda^2)\,, \\ P_6(z) - 2\Lambda^6 &= (z^2 + g + \Lambda^2)^2(z^2 + g - 2\Lambda^2)\,. \end{aligned}$$

These polynomials are obtained by the "multiplication by 3" map; modulo phase factors, $P_6(z)$ in (5.11) is given in terms of $P_2(z) = z^2 + g$ as

$$(5.12) \qquad\qquad P_6(z) = 2\Lambda^6\, T_3\left(\frac{P_2(z)}{2\Lambda^2}\right).$$

The trees in this branch will therefore have confinement index 3.

5.1.2.1. The rigid quartic factorization.   One can set $g = \Lambda^2$ to get the quartic factorization (5.4), whereas one can rescale z to set $\Lambda = 1$. The resulting polynomials that solve (5.4) are

$$(5.13) \qquad \begin{aligned} P_6(z) &= z^4(z^2 + 3) - 2\,, \quad H_2(z) = (z^2 + 2)\,, \\ Q_1(z) &= z \quad \text{and} \quad F_4(z) = (z^2 + 3)(z^2 - 1)\,. \end{aligned}$$

Plotting the roots of the polynomials leads, this time, to the tree in figure 13. The polynomials are defined over $\mathbb{Q}$ and so the tree is the only element in its Galois orbit.

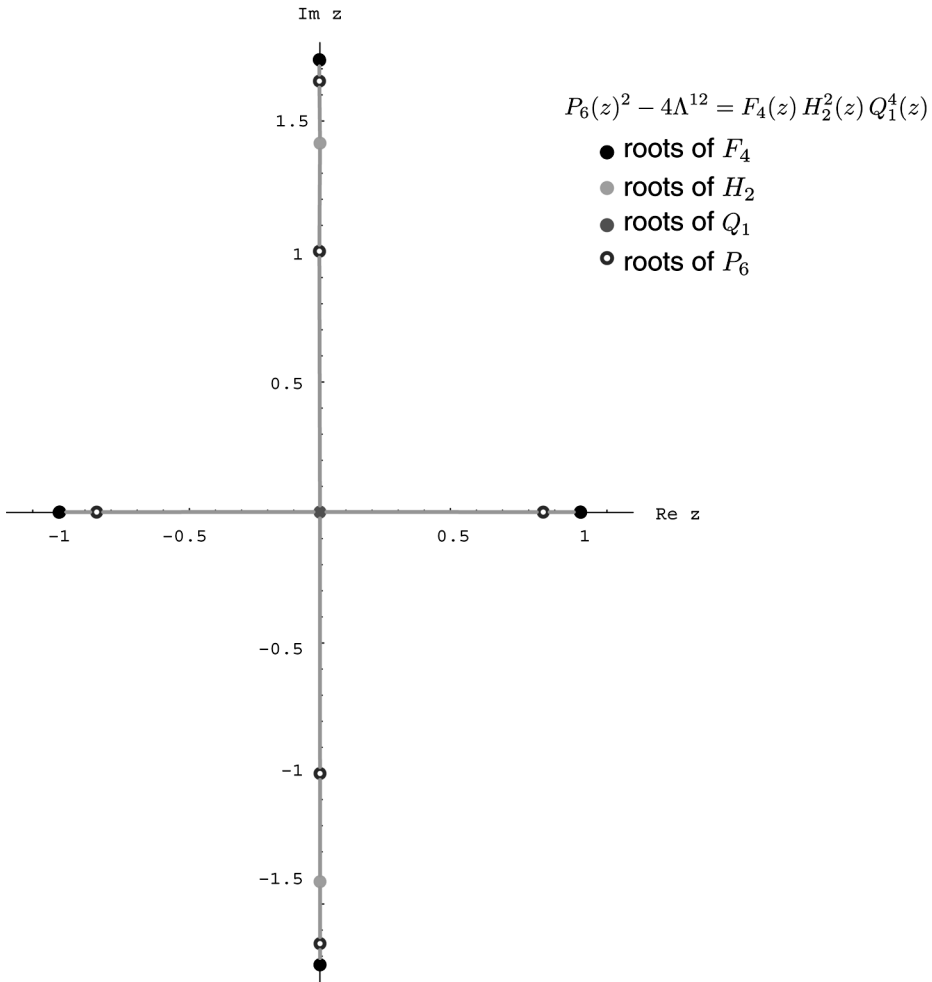[18] Refer Equation (3.50) in [8].

Figure 13: The tree obtained in the $(2, 2)$ confining branch with a four-valent vertex. It has confinement index $t = 3$.

5.1.2.2. The rigid cubic factorization.   Note that it is not possible to get the cubic factorization equation (5.9) by tuning the available free parameter. Thus, we do not find any trivalent tree in this branch of the moduli space. One can also show this using the combinatorial definition of the confinement index by trying to construct a trivalent tree with six edges and $t = 3$.

5.1.3. The (2,2) coulomb vacua.   The solution of the factorization problem (5.4) in this branch is parametrized as[19]

(5.14)

$$P_6(z) + 2\Lambda^6 = \left[z^2 + (1+\sigma)z + \frac{(3+\sigma)(9+15\sigma-\sigma^2+\sigma^3)}{108}\right]^2$$
$$\left[z^2 - \frac{(1-\sigma)(3-\sigma)^2(3+\sigma)}{108}\right]$$

$$P_6(z) - 2\Lambda^6 = \left[\left(z+\frac{2\sigma}{3}\right)^2(1-\sigma)\left(z+\frac{2\sigma}{3}\right) + \frac{(3-\sigma)(9-15\sigma-\sigma^2-\sigma^3)}{108}\right]^2$$
$$\left[\left(z+\frac{2\sigma}{3}\right)^2 - \frac{(1+\sigma)(3+\sigma)^2(3-\sigma)}{108}\right]$$

with σ and Λ satisfying the constraint

(5.15)
$$\sigma^5(\sigma^2-9)^2 = 27^3\Lambda^6.$$

5.1.3.1. The rigid quartic factorization.   Requiring that the first factor in the either of the two equations in (5.14) has a double root leads to the quartic factorization (5.4). We get the condition

(5.16)
$$\sigma^2 - 25 = 0.$$

For $\sigma = 5$, the polynomials that solve the Equation (5.7) are given by

(5.17)
$$Q_1(z) = z - 2, \quad H_2(z) = z^2 - \frac{2}{3}z + \frac{128}{27},$$
$$F_4 = \left(z^2 + \frac{64}{9}\right)\left(z^2 - \frac{20}{3}z + \frac{332}{27}\right),$$
$$P_6(z) = z^6 - 8z^5 + \frac{280}{9}z^4 - \frac{800}{9}z^3 + \frac{560}{3}z^2 - \frac{2048}{9}z + \frac{3,839,488}{19,683}.$$

Plotting the zeroes of the polynomials lead to the tree in figure 14. Since the tree is found in the Coulomb branch, it has confinement index 1. This can also be checked directly using the combinatorial definition: we get $t = \mathrm{GCD}(3,4) = 1$. For $\sigma = -5$, we get an equivalent tree but reflected about

---

[19] Refer to Equation (3.53) in [8]. We have set $g \to \sigma h$, $z- \to z h$ and $\Lambda \to \Lambda h$ in that equation.

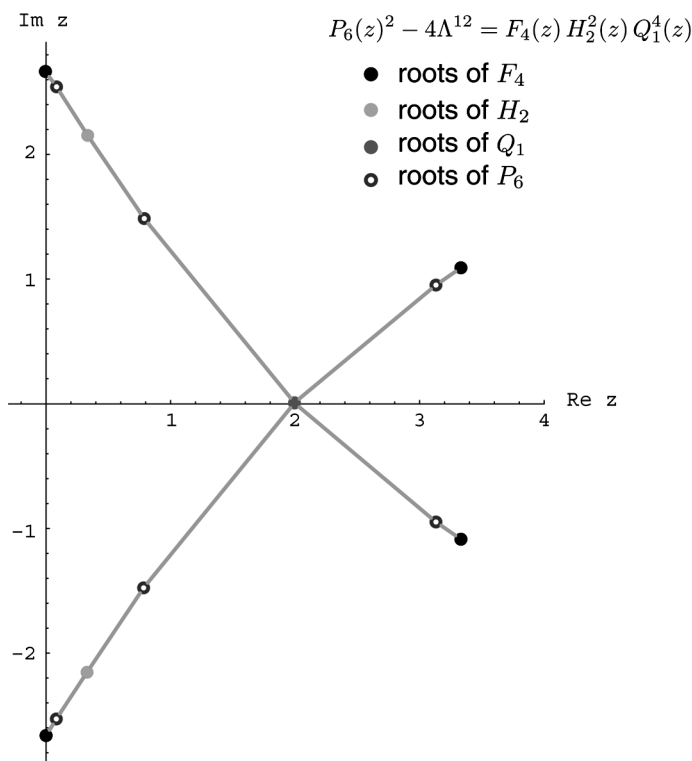Figure 14: The tree obtained in the $(2, 2)$ coulomb branch with a four-valent vertex.

the Re $(z) = 0$ axis. Note that the solution in (5.17), like the ones we have obtained earlier, are polynomials defined over $\mathbb{Q}$. This is why the Galois orbits in each case consist of only a single tree. We now discuss a set of trees whose associated number field is non-trivial and therefore constitute a larger Galois orbit.

5.1.3.2. The rigid cubic factorization.   Requiring that the two factors in the first of the two equations in (5.14) have a root in common leads to the non-trivial condition[20]

$$(5.18) \qquad\qquad \sigma^3 - 3\sigma^2 + 3\sigma + 15 = 0\,.$$

---

[20] The similar constraint for the second equation does not change the number field and we get the same set of trees.

Solving for σ leads to three solutions

(5.19)
$$\sigma = \begin{cases} \sigma^{(0)} = (1 - 2\,(2)^{1/3}), \\ \sigma^{(+)} = (1 + 2^{1/3}(1 - i\,\sqrt{3})), \\ \sigma^{(-)} = (1 + 2^{1/3}(1 + i\,\sqrt{3})). \end{cases}$$

Substituting these results into the polynomials and plotting their roots lead to the trees in figures 15, 16 and 17, respectively. All of these have confinement index $t = 1$.

From the fact that all three trees are obtained from a single polynomial (5.18) irreducible over $\mathbb{Q}$, it follows that these three trees belong to the same Galois orbit. From (5.19), we observe that unlike the earlier solutions which were all defined over $\mathbb{Q}$, the number field associated to these trees is non-trivial.

Let us study this example in more detail. The terminology is explained in Appendix A. By inspection of (5.19), we find that $\sigma^{(0)}$ and $\sigma^{(\pm)}$ belong to the field $K = \mathbb{Q}(2^{1/3}, \omega)$ where $\omega = \frac{1}{2}(1 + i\sqrt{3})$ (a cube root of unity). It is easy to see that K is also the splitting field of the polynomial $x^3 - 2$, whose associated Galois group $\mathrm{Gal}(K/\mathbb{Q})$ is the group of permutations of three elements, S_3, which is non-abelian.
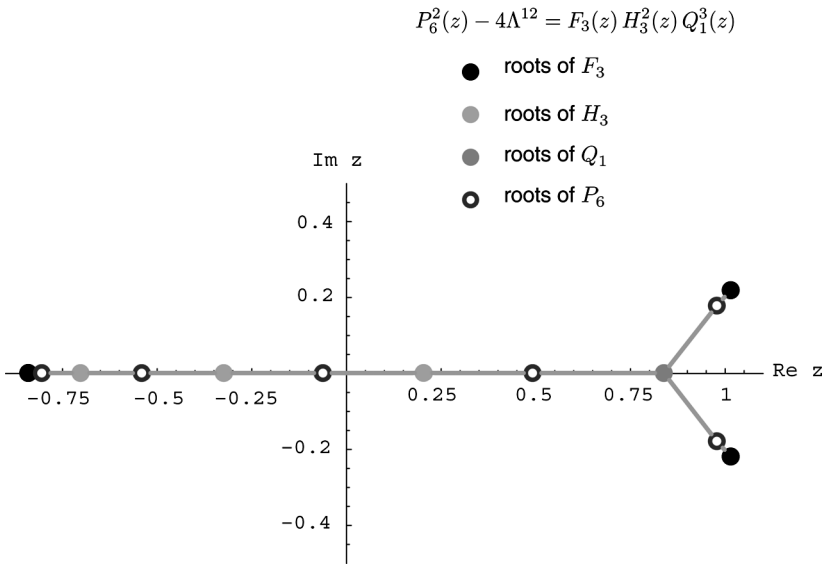
$$P_6^2(z) - 4\Lambda^{12} = F_3(z)\,H_3^2(z)\,Q_1^3(z)$$

Figure 15: Tree for the case $\sigma^{(0)}$ in (5.19). It has $t = 1$.

Sujay K. Ashok, Freddy Cachazo, and Eleonora Dell'Aquila

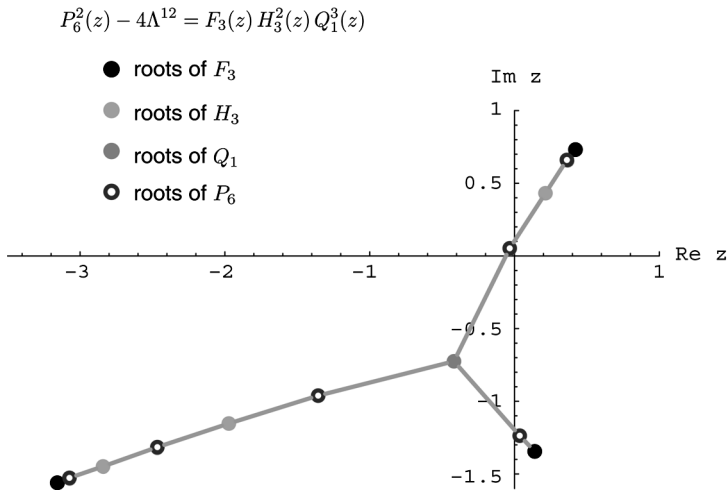$$P_6^2(z) - 4\Lambda^{12} = F_3(z) H_3^2(z) Q_1^3(z)$$

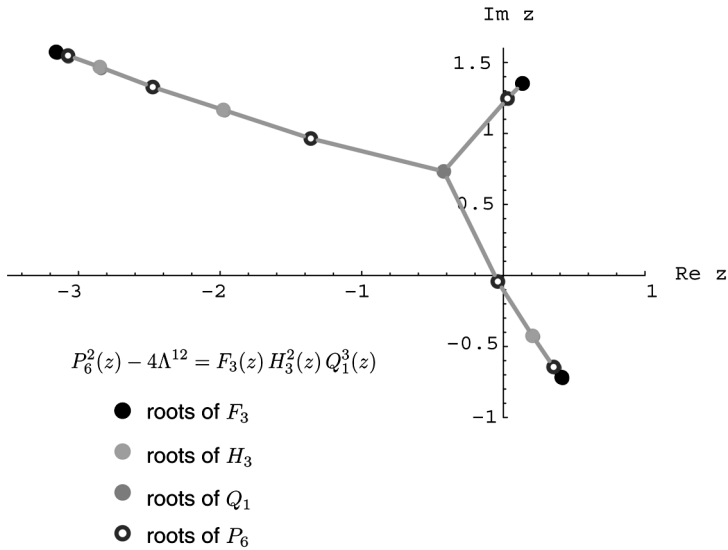Figure 16: Tree for the case $\sigma^{(-)}$ in (5.19). It has $t = 1$.

Figure 17: Tree for the case $\sigma^{(+)}$ in (5.19). It has $t = 1$.

5.1.4. The (3, 2) and (2, 3) vacuum. If two roots of $F_4(z)$ coincide in (5.1) we get the factorization problem

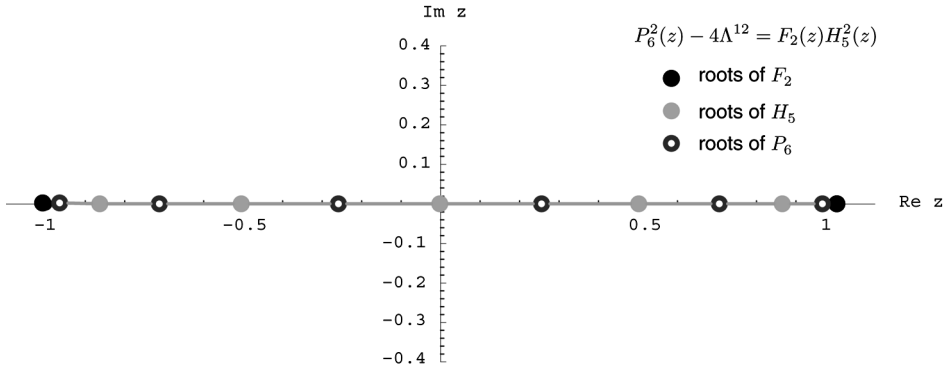(5.20) $$P_6^2(z) - 4\Lambda^{12} = F_2(z) H_5^2(z) = (z^2 - 4\Lambda^2) H_5^2(z),$$

Figure 18: The tree obtained at the maximally confining point. It has $t = 6$.

where, in the second equality, we have suitably shifted and scaled z. Setting Λ to one, (5.20) is solved by the polynomials [12]

$$P_6(z) = 2\, T_6\left(\frac{z}{2}\right) \quad \text{and} \quad H_5(z) = U_5\left(\frac{z}{2}\right) .$$

Plotting the zeroes of these polynomials leads to the branchless tree discussed in Section 2.8. In figure 18, we show the tree that arises for the particular case of $U(6)$. As explained in the earlier more general discussion, this is the singularity at which the $\mathcal{N} = 1$ branches meet. This is the only case we consider that has one of the $N_i = 0$. Therefore, this can be explained as the intersection of $U(1)$ and $U(1)^2$ branches. See Appendix C for a more complete discussion. From the combinatorial definition of the confinement index, the dessin has $t = 6$, the largest value for the case with $N = 6$ edges.

5.2. Classifying dessins from gauge theory

So far, we have started with the non-rigid factorization problem and tuned the parameters to get isolated singularities where dessins appear. We have seen how the dessins fall into different Galois orbits. We now classify them according to the $\mathcal{N} = 1$ branches to which they belong using gauge theory order parameters. We summarize all our findings from the gauge theory point of view in figure 19. Given that the confinement index is a Galois invariant, we find each of the three trees with a four-valent vertex to belong to distinct Galois orbits as shown in figure 19. Similarly, using the confinement index, we find that the trivalent trees fall into at least two distinct Galois orbits: the trivalent dessin with $t = 2$ is left invariant under the action of $\mathrm{Gal}(\overline{\mathbb{Q}}/\mathbb{Q})$.
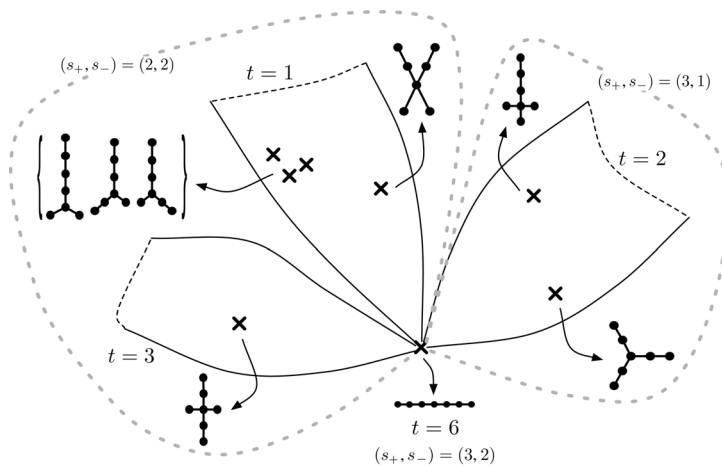
Figure 19: Summary of the analysis of the $U(6)$ gauge theory and the location of the trees in the various branches of the gauge theory moduli space. The dotted lines indicated a coarse-grained classification of $\mathcal{N} = 1$ branches based on the (s_+, s_-) values. In this case, the branches are more finely distinguished by the confinement index t. Branches meet at the point where another monopole becomes massless.

Note that in the $t = 1$ and $t = 2$ branches we have both trivalent and quartic dessins. From our discussion about valency lists, it follows that they are in distinct Galois orbits. However, in each case, they have the same value of t and of (s_+, s_-). This is where extra gauge theory criteria are needed in order to distinguish these isolated phases.

Let us concentrate on the pair of dessins with $t = 2$. A simple way to see that these correspond to two different phases is by tracing them back to the problem in $U(3)$ broken to $U(1) \times U(2)$ and then "multiplying by 2". The trivalent dessin comes from the unique dessin with three edges. Such a special point is where $P_3^2(z) - 1 = z^3(z^3 - 1)$. This is actually known to be a superconformal field theory in the IR (see [13, 24] and references therein). On the other hand, the quartic dessin comes from a generic point in the $U(3)$ theory and therefore it is a different phase.

This discussion proves that the two dessins are in different phases. However, we want to go further and show that even the theory corresponding to the quartic dessin is a distinct phase from its neighbors in the $t = 2$ branch. Recall that in Section 4.2, we argued that there might be extra chiral ring relations that characterize the corresponding special points within each branch. Let us see this in detail in this case.

For the quartic factorization (5.4) in the branch defined by $s_+ = s_- = 2$, we take

$$(5.21) \quad \widetilde{H}_2(z) = (z - c)^2, \quad R_2(z) = z^2 + \alpha z + \beta, \quad H_2(z) = z^2 + \gamma z + \delta.$$

where we have adopted the notations in (3.4). Using these in the definition of the t_r in Section 3.2, we find the following chiral ring relation that is satisfied *only* at the special (quartic) point in the $\mathcal{N} = 1$ branch:

$$
\begin{aligned}
(5.22) \quad & 4\, t_0\, t_2^3 - 3\, t_1^2\, t_2^2 + 4\, t_1^3\, t_3 - 6\, t_0\, t_1\, t_2\, t_3 + t_0^2\, t_3^2 - 4t_1^3\, \Lambda^6 + 6\, t_0\, t_1\, t_2\, \Lambda^6 \\
& - 2t_0^2\, t_3\, \Lambda^6 + t_0^2\, \Lambda^{12} = 0.
\end{aligned}
$$

Note that this relation uses the Λ^6 term in (3.6). In this polynomial, each term has the same R-charge, or equivalently the same dimension, and also the same Q_Φ. To see this, note that Λ naturally has $Q_\Phi = 1$. However, in (5.22) we have set the coupling of the cubic term in the superpotential to 1. Such a coupling g is dimensionless, has $Q_\Phi = -3$ and shows up in (5.22) in the combination $g\Lambda^6$ which then has $Q_\Phi = 3$.

Our new relation (5.22) is not satisfied at any other point in the $t = 2$ branch apart from the special point under consideration. At any other point in the same branch one can show that all t_r's with $r = 0, \ldots, 5$ are independent. In other words, one can at most find a relation similar to (5.22), which gives t_6 in terms of the other six. Assuming that our conjectures about the physical order parameters being Galois invariants are correct, this concludes our discussion of the trees from the physics point of view as we have, using purely gauge theory criteria, managed to classify the dessins into distinct Galois orbits.

5.3. $U(6)$ gauge theory: a mathematician's point of view

We now exhibit how a mathematician would tackle the same problem of classifying dessins into Galois orbits. We start with a particular valency list and find all solutions to the associated polynomial equations using differentiation methods. In the end, one generically finds a polynomial that factors over $\mathbb{Q}$. Each factor corresponds to a different Galois orbit.

For the $U(6)$ gauge theory perturbed by a cubic superpotential, there are three distinct valency lists possible for the rigid factorization problem:

- Consider the branchless tree shown in figure 18. From the valency list, one gets the polynomial equation

$$(5.23) \qquad P_6^2(z) - 4 = F_2(z)H_5^2(z) = (z^2 - 4)H_5^2(z),$$

where, in the second equality, we have suitably shifted and scaled z. In Appendix A of [16], we have already shown how to obtain the solution to this equation using the differentiating trick. The solutions are Chebyshev polynomials. Plotting the roots of the polynomials, we get back the tree in figure 18.

- The trees shown in figures 11, 13 and 14 have the same valency list and arise from the polynomial equation

$$(5.24) \qquad P_6(z)^2 - 4 = F_4(z)\, H_2^2(z)\, Q_1^4(z).$$

Differentiating (5.24) we get

$$(5.25)$$
$$2\, P_6(z)P_6'(z) = H_2(z)\, Q_1^3(z)(F_4'(z)H_2(z)Q_1(z) + 2\, F_4(z)H_2'(z)Q_1(z)$$
$$+ 4\, F_4(z)H_2(z)Q_1'(z)).$$

Since all polynomials involved are monic, it is easy to see that this leads to two equations

$$(5.26)$$
$$P_6'(z) = 6\, H_2(z)\, Q_1^3(z),$$

$$12\, P_6(z) = F_4'(z)H_2(z)Q_1(z) + 2\, F_4(z)H_2'(z)Q_1(z) + 4\, F_4(z)H_2(z)Q_1'(z).$$

After scaling and shifting the z variable, one can write

$$H_2(z) = z^2 - 1, \quad Q_1(z) = z + q_1,$$

$$(5.27)$$
$$P_6(z) = z^6 + \sum_{i=1}^{6} p_i\, z^{6-i}, \quad F_4(z) = z^4 + \sum_{i=1}^{4} f_i\, z^{4-i}.$$

The first equation in (5.26) leads to linear equations for the p_i, which we can easily solve to obtain

$$(5.28) \qquad p_1 = \frac{18}{5}q_1, \quad p_2 = \frac{3}{2}(3q_1^2 - 1),$$
$$p_3 = 2q_1(q_1^2 - 3), \quad p_4 = -9q_1^2, \quad p_5 = -6q_1^2.$$

Substituting this in the second of the two equations in (5.26) leads to

$$(5.29) \quad f_1 = \frac{16}{5} q_1, \quad f_2 = \frac{1}{25}(79 q_1^2 - 25), \quad f_3 = \frac{2}{25} q_1 (7 q_1^2 - 55),$$
$$f_4 = \frac{1}{100}(-75 - 718 q_1^2 - 35 q_1^4), \quad p_6 = \frac{1}{100}(25 + 276 q_1^2 + 7 q_1^4),$$

such that q_1 satisfies the equation

$$(5.30) \qquad\qquad q_1(q_1^2 - 25)(5 q_1^2 + 3) = 0.$$

Each inequivalent solution of (5.30) leads to a dessin. Thus, each dessin has associated to it a specific number field [15]. In (5.30), there are solutions obtained by an overall sign flip: these do not lead to inequivalent trees.

Plotting the roots of the polynomials for each of the cases $q_1 = \{5, 0, i\sqrt{\frac{3}{5}}\}$, respectively, leads to the trees in figures 11, 13 and 14. Since each of the values of q_1 is a Galois orbit in itself (up to an overall sign), the three solutions lead to dessins that belong to different Galois orbits. Thus, they should have a different set of Galois invariants. That this is so can be checked by computing the monodromy groups. We will postpone further analysis to the discussion in Section 5.3.

- The trivalent trees in figures 12, 15, 16 and 17 all have the same valency list and arise from the polynomial equation

$$(5.31) \qquad\qquad P_6^2(z) - 4 = F_3(z) H_3^2(z) Q_1^3(z).$$

Differentiating the equation as before leads to two equations
(5.32)
$$P_6'(z) = 6 H_3(z) Q_1^2(z),$$
$$12 P_6(z) = F_3'(z) H_3(z) Q_1(z) + 2 F_3(z) H_3'(z) Q_1(z) + 3 F_3(z) H_3(z) Q_1'(z).$$

We can choose to parametrize the polynomials as

$$P_6(z) = z^6 + \sum_{i=1}^{6} p_i z^{6-i}, \quad H_3(z) = z^3 + \sum_{i=1}^{3} h_i z^{3-i},$$
$$(5.33)$$
$$Q_1(z) = z, \quad F_3(z) = z^3 + \sum_{i=1}^{3} f_i z^{3-i},$$

where we have used the shift symmetry to set the constant coefficient of Q_1 to be zero. We will not discuss the solution in detail here, as the analysis

is similar to the one we did for the quartic factorization. The solution set is parametrized by (h_1, h_2) that satisfy the relation

$$(5.34) \qquad 24\, h_1^6 - 156\, h_1^4\, h_2 + 450\, h_1^2\, h_2^2 - 625\, h_2^3 = 0\,.$$

We find two branches of solutions:

(a) $h_1 = h_2 = 0$: This leads to the simple solutions

$$(5.35) \quad P_6(z) = z^6 + 2z^3 + \frac{1}{2}\,, \quad H_3(z) = z^3 + 1\,, \quad f_3(z) = z^3 + 2\,.$$

The tree that corresponds to this solution is shown in figure 12.

(b) $h_1, h_2 \neq 0$: One can use the scaling symmetry to set $h_1 = 1$ and there are three solutions which are solutions to the cubic equation for h_2 in (5.34). These are given by
(5.36)

$$h_2 = \begin{cases} h_2^{(0)} = -\dfrac{2}{25}(-3 - 2\,(2)^{1/3} + 2^{2/3})\,, \\[2mm] h_2^{(+)} = \dfrac{1}{25}(6 + 2^{2/3}(1 - i\,\sqrt{3}) - 2\,(2)^{1/3}(1 + i\,\sqrt{3}))\,, \\[2mm] h_2^{(-)} = \dfrac{1}{25}(6 + 2^{2/3}(1 + i\,\sqrt{3}) - 2\,(2)^{1/3}(1 - i\,\sqrt{3}))\,. \end{cases}$$

The three trees associated to $h_2^{(0)}$, $h_2^{(-)}$ and $h_2^{(+)}$ are shown in the figures 15, 16 and 17, respectively. Since $h_2^{(0)}$, $h_2^{(\pm)}$ are solutions to the polynomial equation (5.34) which is irreducible over $\mathbb{Q}$, the corresponding dessins are part of the same Galois orbit. Moreover, the number field is $\mathbb{Q}(2^{1/3}, w)$ with $w^3 = 1$ as it should be from our discussion in Section 5.1.

For $h_2 = h_2^{(0)}$ (figure 15), we present the polynomials that solve (5.32):
(5.37)

$$P_6(z) = z^6 + \frac{6}{5}z^5 + \frac{11,250 + 7500(2)^{1/3} - 3750(2)^{2/3}}{31,250} z^4$$

$$+ \frac{1000 + 4500(2)^{1/3} - 3000(2)^{2/3}}{31,250} z^3 + \frac{44 + 30(2)^{1/3} - 51(2)^{2/3}}{31,250}\,,$$

$$H_3(z) = z^3 + z^2 + \frac{30 + 20(2)^{1/3} - 10(2)^{2/3}}{125} z + \frac{2 + 9(2)^{1/3} - 6(2)^{2/3}}{125}\,,$$

$$F_3(z) = z^3 + \frac{2}{5}z^2 + \frac{-15 + 20(2)^{1/3} - 10(2)^{2/3}}{125} z + \frac{8 - 6(2)^{1/3}}{125}\,.$$
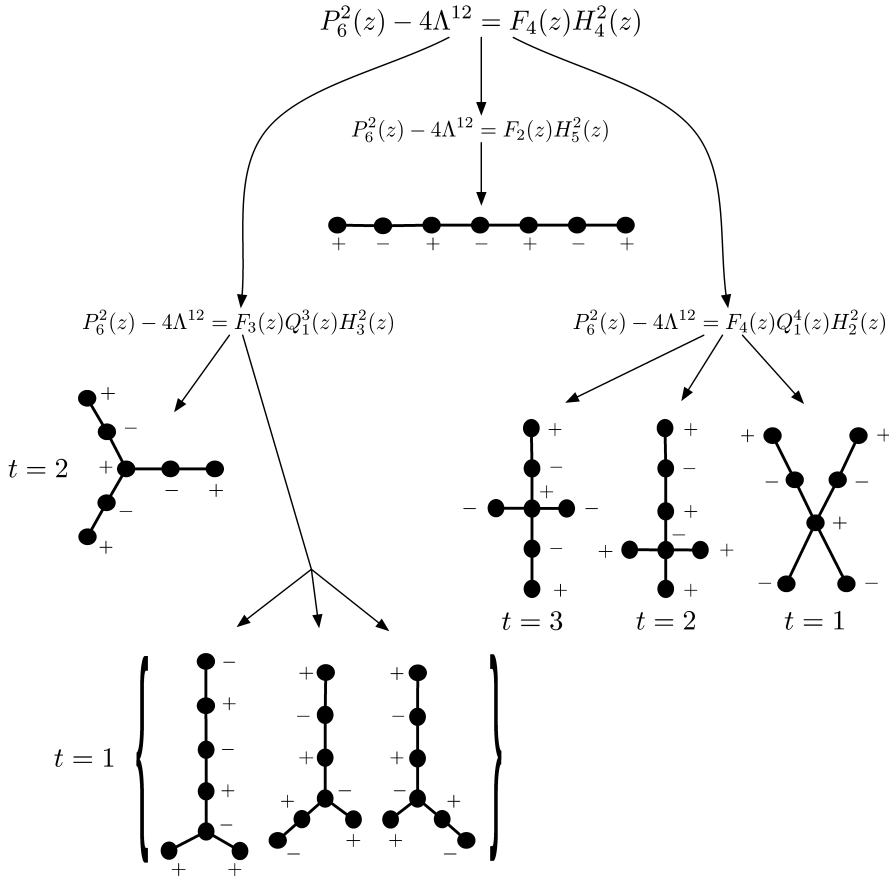
Figure 20: Summary of the analysis of the $U(6)$ gauge theory and the associated dessins. We have also included the results of gauge theory analysis and indicated the confinement index and refined valency list of each figure.

By direct computation, we have therefore classified into Galois orbits the class of trees with six edges that we considered in Section 5.1. The results of the mathematical analysis of the rigid factorizations are summarized in figure 20. These coincide with the classification we obtained from the gauge theory analysis.

5.4. Using galois invariants to classify dessins

In the previous section, we have shown explicitly how dessins are organized into Galois orbits. We now attempt to rediscover the classification using the

Galois invariants discussed in Section 3.1, focusing on the factorizations in (5.24) and (5.31).

5.4.1. Quartic case. From the direct solution of the factorization problem, we see that there are three distinct Galois orbits that correspond, respectively, to the three distinct trees in figures 11, 13 and 14. These three trees can be partially distinguished by the more refined valency list introduced in Section 2.6 for trees. Let us see this in detail.

Depending on how one distributes the roots between the two factors $(P(z) \pm 2)$, there are two distinct possibilities:

$$(5.38) \qquad P_6(z) - 2 = \begin{cases} \widetilde{H}_1^2(z) Q_1^4(z), \\[2ex] F_2(z) Q_1^4(z). \end{cases}$$

If we assign negative valences to each of the zeroes of the polynomials appearing on the right, then, the first choice singles out the tree in figure 13 as the only possibility. On the other hand, the second possibility is satisfied by the trees in both figures 11 and 14. We assign signs $+/-$ to the vertices in figure 20 to indicate these two possibilities.

In order to distinguish the remaining two dessins, we can compute the monodromy group of the trees[21]. Here, we compute the monodromy groups of the trees with the refined bi-partite structure, as in figure 8 of Section 2.6. Taking the difference of the two equations in (2.14) we find an auxiliary polynomial equation that leads to a non-clean Belyi map, whose pre-images of 1 are the vertices with — valency and whose pre-images of 0 are vertices with + valency. The monodromy group for trees is therefore generated by $\sigma_{+/-}$, which correspond to the permutation of edges around the $+/-$ vertices, respectively.

The groups of all the trees we have encountered in the $U(6)$ example have been collected in Table 1. S_n is the permutation group of n elements whereas C_n is the cyclic group of n elements. The monodromy group turns out to be different for the trees in figures 11 and 14: for figure 11, we get the monodromy group $(S_3 \times S_3) \ltimes C_2$, of order 72, whereas for figure 14, we get the monodromy group S_5, of order 120.

---

[21] All the monodromy groups have been obtained using the GAP software downloaded from http://www.gap-system.org.

Table 1: Monodromy groups for dessins that occur in the pure $U(6)$ gauge theory perturbed by a cubic superpotential.

Figures	Monodromy group
11	$(S_3 \times S_3) \ltimes C_2$
13	$C_2 \times S_4$
14	S_5
12	$C_3 \times S_3$
15, 16, 17	S_6

5.4.2. Cubic case. The discussion parallels the one for the quartic factorization. The two possibilities of distributing the roots

$$(5.39) \qquad P_6(z) - 2 = \begin{cases} F_3(z)Q_1^3(z), \\ F_2(z)\widetilde{H}_2^2(z), \end{cases}$$

correspond to two distinct refined valency lists that distinguishes the tree in figure 12 from any one of the trees in figures 15, 16 or 17. In this case, no further invariant is required to distinguish them.

Thus, we find that the classification of dessins into Galois orbits agrees with what we obtained in Section 5.2 regarding the classification of isolated phases in gauge theory. So far, we have only considered dessins that are trees. We now generalize our discussion and consider more general dessins. This will highlight some open questions related to the phases of gauge theories with flavour.

6. Gauge theories with flavour

In this section, we turn to a discussion of gauge theories with matter. The dessins that appear at isolated singularities in the moduli space will no longer be trees. We will mostly focus on the curves that were discussed in [16], with isolated Argyres–Douglas singularities in the moduli space.

We start with a general discussion of the non-rigid factorization

$$(6.1) \qquad P_N^2(z) + B_L(z) = Q_{2n}(z)H_{N-n}^2(z) \,,$$

where we have exhibited the degrees of the polynomials explicitly. This curve arises from a $\mathcal{N} = 2$ $U(N)$ gauge theory with N_f massive flavors broken to $\mathcal{N} = 1$ by a tree level superpotential

$$(6.2) \qquad W_{\text{tree}} = \text{Tr}\,W(\Phi) + \widetilde{Q}_{\widetilde{f}} m_f^{\widetilde{f}}(\Phi) Q^f \,,$$

where f and $\widetilde{f}$ run over the number of flavors N_f and

$$(6.3) \qquad W(z) = \sum_{k=1}^{n+1} \frac{g_k}{k} z^k, \quad m_f^{\widetilde{f}}(z) = \sum_{k=1}^{l+1} m_{f,k}^{\widetilde{f}} z^{k-1}.$$

The $\mathcal{N} = 1$ vacua, as before, are those for which $Q_{2n}(z) = W'(z)^2 + f(z)$, where $f(z)$ is a polynomial such that $\deg(f) = \deg(W'(z))/2 - 1$. $m(z)$ is a matrix of polynomials of size $N_f \times N_f$.

It turns out that the only information about the superpotential $\widetilde{Q}_{\widetilde{f}} m_f^{\widetilde{f}}(\Phi) Q^f$ which is relevant for the curve (6.1) is the polynomial [25, 26, 9]

$$(6.4) \qquad B_L(z) = \det m(z).$$

Clearly, plenty of choices of $m(z)$ can lead to the same $B_L(z)$.

The particular class of dessins we are interested in arise when $B_L(z)$ has only $n+1$ distinct roots. We use our shift and scale symmetry to set $B_L(z)$ to be of the form

$$(6.5) \qquad B_L(z) = \alpha \, z^{m_0} (z-1)^{m_1} \prod_{j=2}^{n} (z - p_j)^{m_j} \,.$$

Two natural ways of obtaining such $B(z)$'s are the following:

- $N_f = L = \deg B_L(z)$ and $m_f^{\widetilde{f}}(z)$ a constant diagonal mass matrix with m_0 masses equal to 0, m_1 masses equal to 1, and m_j masses equal to p_j.
- $N_f = n+1$ and $m_f^{\widetilde{f}}(z)$ a diagonal matrix with polynomial entries z^{m_0}, $(z-1)^{m_1}$, and $(z-p_j)^{m_j}$.

The former leads to a theory with unbroken $\mathcal{N} = 2$ supersymmetry, if there is no $W(z)$. Moreover, it has a large flavor symmetry classically. The latter, on the other hand, has a very small number of flavors and generically no special flavor symmetry.

What we now do to obtain the Argyres–Douglas (AD) dessins studied in [16] is to further tune the masses of the flavors and the parameters of the superpotential to set

$$(6.6) \qquad H_{N-n}(z) = Q_{2n}(z) \, R_{N-3n}(z) \,.$$

This leads to the rigid factorization problem [16]

$$(6.7) \qquad P_N^2(z) + B_L(z) = Q_{2n}^3(z) \, R_{N-3n}^2(z) \,.$$

We will focus on such factorizations in the rest of the section since many explicit solutions to this class of factorization problems have already been obtained in [16]. We will exploit these solutions to discuss some interesting issues in gauge theory.

6.1. $U(10)$ gauge theory with flavour

Consider the specific case of dessins arising from the factorization problem of the second example in Section 2.3:

$$(6.8) \qquad P_{10}^2(z) + \alpha z^5(z-1)^5(z-t)^5 = Q_4^3(z)R_4^2(z).$$

This problem was completely solved in [16]. There are two inequivalent solutions to (6.8). Borrowing the explicit solutions from [16] one can plot the zeroes of the polynomials as before; we have drawn the corresponding dessins in figures 21 and 22.

It turns out that the monodromy group distinguishes between the two dessins and therefore they belong to different Galois orbits. For the two dessins considered here, the relations $\sigma_1^2 = 1$ and $\sigma_0^6 = 1$ are satisfied. Let us denote the two monodromy groups corresponding to the two dessins by M_1 and M_2, respectively. In order to explicitly write down the generators, it is useful to number the half-edges of the dessin, as in the figures 21 and 22.

From the definitions, one can check that

— M_1 is generated by

$$(6.9)$$
$$\sigma_1 = (1,2)(3,4)(5,6)(7,8)(9,10)(11,12)(13,14)(15,16)(17,18)(19,20),$$

$$\sigma_0 = (1,10,11)(2,15,3)(4,5)(6,19,7)(8,9)(12,13)(14,20,18)(16,17).$$

It has order $30,720$ and has 84 conjugacy classes.

— M_2 is generated by

$$(6.10)$$
$$\sigma_1 = (1,2)(3,4)(5,6)(7,8)(9,10)(11,12)(13,14)(15,16)(17,18)(19,20),$$

$$\sigma_0 = (1,10,11)(2,13,3)(4,19,5)(6,7)(8,9)(12,20,18)(14,15)(16,17).$$

It has order $30,720$ and has 63 conjugacy classes.

Since $M_1 \neq M_2$, the two dessins belong to distinct Galois orbits. We can now ask if it is possible, from the gauge theory analysis, to distinguish between them. Note that the holomorphic invariants introduced in Section 3.2 do not give any information in this case, as it is not possible to factorize
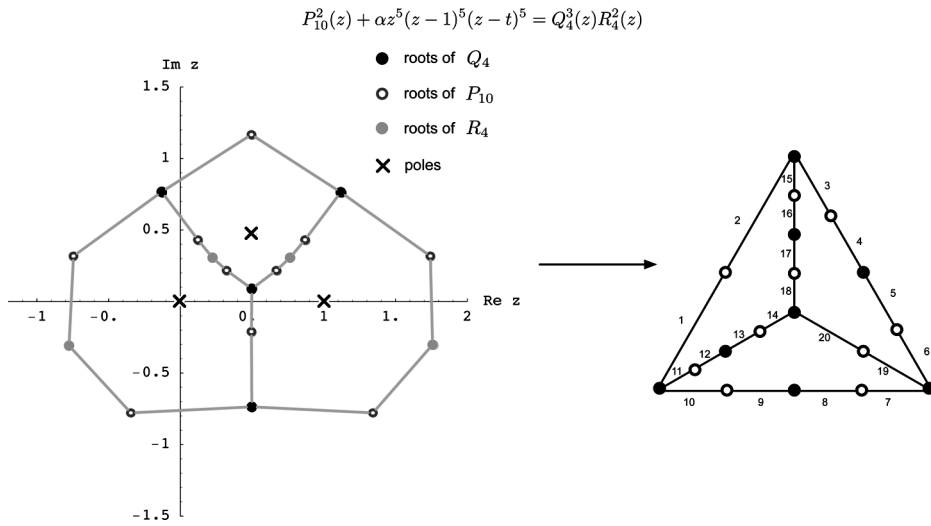
$$P_{10}^2(z) + \alpha z^5(z-1)^5(z-t)^5 = Q_4^3(z)R_4^2(z)$$

Figure 21: One of the two dessins arising from the factorization (6.8). Each face is bounded by three line segments containing $1, 2$ and 2 edges, respectively. The figure to the right is a schematic version of the dessin, with the edges numbered to aid the computation of the monodromy group.
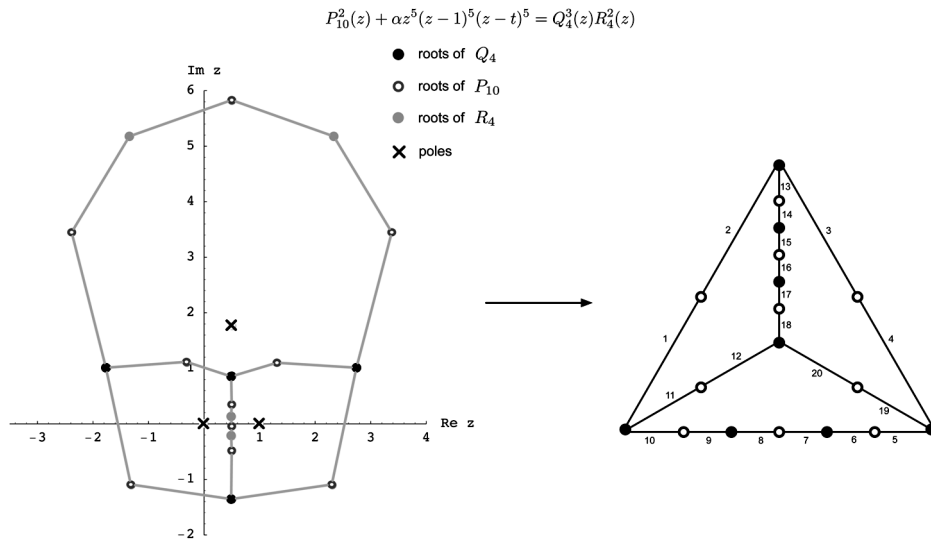
$$P_{10}^2(z) + \alpha z^5(z-1)^5(z-t)^5 = Q_4^3(z)R_4^2(z)$$

Figure 22: The other dessin arising from (6.8). Each face is bounded by $1, 1$ and 3 edges between trivalent vertices.

(6.8) as $P(z) \pm f(z)$, for some polynomial $f(z)$, unlike the pure gauge theory case. This is reflected in the fact that from the mathematical point of view, it is not possible in general to define a refined valency list when the dessin is not a tree.

Similarly, although the combinatorial definition of the confinement index still makes sense, there is no sense in which confinement is a good order parameter for gauge theories with matter. So although t might still be a good Galois invariant, its physical interpretation is unclear. Some preliminary analysis of the phases have already been attempted in [27]. We leave a more detailed study of theories with flavor for future work.

7. Conclusions and open questions

The central theme of this work has been the relation between dessins d'enfants and supersymmetric gauge theory. In this section, we discuss some of the results we have obtained and list some of the immediate questions and future directions of research that have emerged from our analysis.

We have seen that any clean dessin with N_c edges and $N_f + 1$ faces can be found at an isolated singularity in the moduli space of an $\mathcal{N} = 2 U(N_c)$ gauge theory with N_f flavours. The particular rigid factorization of the Seiberg–Witten curve that corresponds to the isolated singularity is determined by the valency lists of the dessin. Typically, there are many solutions to this factorization problem. For each such solution, the rigid curve determines a rational Belyi map $\beta(z)$ whose inverse image of the $[0, 1]$ interval gives a dessin D on the sphere. Such an $\mathcal{N} = 2$ gauge theoretic perspective matches very closely the mathematical point of view of obtaining and classifying dessins into Galois orbits by direct solution of the polynomial equation.

From a physics point of view, it is also natural to study what we called the non-rigid factorizations (1.2). The solutions to these equations are interpreted as the space of vacua that preserve $\mathcal{N} = 1$ supersymmetry when the $\mathcal{N} = 2$ theory is perturbed by a tree level superpotential. One can associate to these vacua disconnected graphs (which are not dessins), that come together and join to form a dessin at any of the isolated singularities mentioned in the previous paragraph. The difference lies in the fact that these are now looked upon as $\mathcal{N} = 1$ vacua.

Interestingly, it is this $\mathcal{N} = 1$ point of view that has a nice counterpart in the more refined mathematical approach to the study of dessins, which is to define a complete list of Galois invariants that distinguish the dessins that belong to different Galois orbits. Based on the examples we have worked out,

we have been led to conjecture a relation between the mathematical program of classifying dessins and the physics program of classifying phases of $\mathcal{N} = 1$ gauge theory. The strongest form of the conjecture states that every Galois invariant is a physical order parameter that distinguishes different phases in the gauge theory.

One example of a Galois invariant that might give new physical information is the monodromy group associated to the dessins. In gauge theory, the group usually discussed in the context of Seiberg–Witten theory is the S-duality group: for a genus g Seiberg–Witten curve, it is an $Sp(2g, \mathbb{Z})$ group that acts on the A_i and B_i cycles of the Riemann surface. These cycles correspond to the edges that go between the filled vertices of the dessins (the pre-images of 0 under the Belyi map). However, in general the monodromy group of the dessin involves action on half-edges that go between the pre-images of 0 and 1 and involves the zeroes of $P(z)$, apart from the zeroes of y_{SW}. It is therefore different from the S-duality group, but what exactly the group signifies in the gauge theory is an open question.

In the other direction, one can ask whether the $\mathcal{N} = 1$ gauge theoretic way of finding the dessins, first by solving a more general (non-rigid) factorization problem and *then* imposing suitable constraints so that one approaches an isolated singularity in the moduli space, is useful from a mathematical point of view. From our proof that the confinement index is a Galois invariant, it seems that the answer is yes. More generally, we have seen that all the order parameters have a simple interpretation in the mathematical literature as Galois invariants. We believe that in this direction the correspondence is on much firmer ground.

In Section 6, we discussed dessins that appear in the moduli space of a $U(N)$ gauge theory with matter. Much less is known about the possible phases of the corresponding $\mathcal{N} = 1$ vacua. We exhibited two dessins in a $U(10)$ theory with flavour, which, from the mathematical point of view belong to distinct Galois orbits as they have different monodromy groups. However, from the physics point of view, with the available order parameters, it seems that the points where the two dessins appear describe the same phase. By this, we mean that none of the known order parameters are of any use to distinguish between them. If our stronger conjecture that Galois invariants map to order parameters is correct, the monodromy group should correspond to an order parameter in physics that can distinguish the two special points where the dessins appear.

Many possible generalizations of our work present themselves. Since the dessins can be drawn on any two-dimensional topological surface, it should be possible to extend the correspondence we have found to dessins drawn on

genus $g \geq 1$ Riemann surfaces. On the gauge theoretic side, it would be very interesting to classify the dessins that appear in the moduli spaces of more general gauge theories, such as SO/Sp gauge groups, quiver gauge theories with products of $U(N)$ factors, etc.

The study of the $\mathcal{N} = 1$ branches in [8] uses the Dijkgraaf–Vafa relation between gauge theory and matrix models [28, 29, 30]. In this relation, two distinct hyperelliptic Riemann surfaces emerge [22]: the Seiberg–Witten curve and the spectral curve of the matrix model. In the examples considered in the text, the spectral curve was equivalent to the reduced Seiberg–Witten curve in (1.4). However, this is not true in general as discussed in the examples in Appendix C. It is conceivable that one can tune the parameters of the tree level superpotential so that the spectral curve develops an isolated singularity, leading to a Belyi map. It might be very interesting to study the dessins that arise this way.

As we have stressed throughout, the main objective of this article was to provide the rudiments of a dictionary between the physics of supersymmetric gauge theory and the mathematics related to the action of the absolute Galois group on the children's drawings of Grothendieck. Much more work needs to be done to fully understand the correspondence between these two fascinating fields of study, which we hope will lead to a deeper and fuller understanding of the relevant physical and mathematical problems.

Acknowledgments

Appendix A. Field theory and the absolute galois group

The main mathematical object that appears in this paper is the absolute Galois group $\mathrm{Gal}(\overline{\mathbb{Q}}/\mathbb{Q})$. It is of central importance in many areas of mathematics. Since this group is not very familiar to physicists, in this appendix we give a short description of the definition stated in the text: $\mathrm{Gal}(\overline{\mathbb{Q}}/\mathbb{Q})$ is

the group of automorphisms of the field $\overline{\mathbb{Q}}$ of algebraic numbers that leaves $\mathbb{Q}$ fixed.

Instead of directly studying $\mathrm{Gal}(\overline{\mathbb{Q}}/\mathbb{Q})$, which is a group that cannot even be finitely generated, we will study the relevant concepts by first reviewing Galois groups of finite order. Just to give an idea of the complexity of $\mathrm{Gal}(\overline{\mathbb{Q}}/\mathbb{Q})$ it is nice to mention that mathematicians are considering the possibility that any finite group can arise as a projection of $\mathrm{Gal}(\overline{\mathbb{Q}}/\mathbb{Q})$; this is the so-called "Inverse Problem of Galois Theory"[22].

Before going into the details about the different elements that enter in the definition of Galois groups let us lay down some field theory basis. In this review, we will assume familiarity with definitions of fields, rings of polynomials and basic group theory (for a very basic introduction and more details of the main example in this appendix see [31]).

Let us start by recalling some basic definitions. We say that a field E is an extension of a field F, denoted by $F \leq E$, if E has a subfield isomorphic to F. Examples of fields and extensions are $\mathbb{Q} \leq \mathbb{Q}(2^{1/4}, i) \leq \overline{\mathbb{Q}}$. Our first goal is to review the meaning of expressions such as $\mathbb{Q}(2^{1/4}, i)$.

Given a field F, a natural object to study is the ring of polynomials, $F[z]$, with coefficients in F. From now on we will assume that F is a field of characteristic zero or a finite field. This is to avoid certain pathologies that can happen otherwise. Of course, our final target, which is $\mathbb{Q}$, has characteristic zero.

An element $a \in E$ is called algebraic over F if it is a zero of a polynomial $p(z)$ in $F[z]$. E is called an algebraic extension of F if all its elements are algebraic over F. We will only consider algebraic extensions from now on. It turns out that there exists a unique monic irreducible (over F) polynomial such that $p(a) = 0$ (since F is of characteristic zero or finite, a can only be a zero of order one. This is an example of one of the possible pathologies we have avoided). Since such a $p(z)$ is unique we call it $p_a(z)$. The degree of $p_a(z)$, $\deg(p_a(z)) = n$ is also called the degree of a in F.

A special class of algebraic extensions are those with the structure of a vector space with basis $\{1, a, \ldots, a^{n-1}\}$ and coefficients in F. These are called *simple extensions* and are denoted by $F(a)$. In general, if $F \leq E$ and E is of finite dimension n as a vector space over F, we say that E is a *finite extension*[23] of degree $|E : F| = n$ over F.

---

[22] The more precise statement is that any simple group S might be the Galois group of a finite normal extension of $\mathbb{Q}$ and hence there will be a natural restriction map from $\mathrm{Gal}(\overline{\mathbb{Q}}/\mathbb{Q})$ onto S.

[23] Quite nicely, in our case (with $F = \mathbb{Q}$), all finite extensions are also simple! This is called the primitive element theorem.

An example is $F = \mathbb{Q}$ and $a = 2^{1/4}$. Then $\mathbb{Q}(2^{1/4})$ is generated by $\{1, 2^{1/4}, 2^{1/2}, 2^{3/4}\}$ since $p_a(z) = z^4 - 2$ has degree $n = 4$.

Note that $z^4 - 2$ is reducible over $\mathbb{Q}(2^{1/4})$, in fact, $z^4 - 2 = (z - 2^{1/4})(z + 2^{1/4})(z^2 + 2^{1/2})$. The last factor, $(z^2 + 2^{1/2})$, is irreducible of degree 2 in $\mathbb{Q}(2^{1/4})$. So if we *adjoin* a root of $z^2 + 2^{1/2}$ to $\mathbb{Q}(2^{1/4})$ then $z^4 - 2$ *splits* over this new field.

The new element we need is $2^{1/4}i$. However, multiplying by $2^{-1/4} \in \mathbb{Q}(2^{1/4})$ we get i. Therefore, the new field is $(\mathbb{Q}(2^{1/4}))(i) = \mathbb{Q}(2^{1/4}, i)$. The latter notation shows the fact that the order in which we adjoin $2^{1/4}$ and i to $\mathbb{Q}$ is irrelevant.

We have achieved our first goal: $\mathbb{Q}(2^{1/4}, i)$ is called the *splitting field* of $z^4 - 2$. More generally, an extension E of $\mathbb{Q}$ is a splitting field if there is an irreducible polynomial in $\mathbb{Q}[z]$ such that E is the smallest field that contains all its roots.

Now we need to introduce the concept of the algebraic closure of a field F. A field K is called algebraically closed if every non-constant polynomial in $K[z]$ has a root in K. Such a K is called an algebraic closure of F if K is an algebraic extension of F, and it is denoted by $\overline{F}$. $\overline{F}$ is unique up to isomorphisms.

The next goal is to study automorphisms of fields. Splitting fields are important because given any one of them, say E such that $F \leq E \leq \overline{F}$, any automorphism of $\overline{F}$ that fixes F maps E onto itself and induces an automorphism of E leaving fixed F. Moreover, splitting fields are the only ones with this property. The basic automorphisms are quite simple: if a and b are roots of the same irreducible polynomial, then the map $\phi(a) = b$ with $\phi(q) = q$ if $q \in F$ is an automorphism. a and b are called conjugates and ϕ is a conjugation. Automorphisms of E that leave fixed F form a group under composition denoted by $G(E/F)$. If E is a splitting field, then $G(E/F)$ is called the Galois group of E over F and it is denoted by $\mathrm{Gal}(E/F)$.

Let E be a finite extension of F. The number of isomorphisms of E into $\overline{F}$ leaving F fixed is the index $\{E : F\}$ of E over F. It turns out that for the fields we consider

$$(A.1) \qquad \{E : F\} = |E : F| = |G(E/F)|,$$

where $|G(E/F)|$ is the order of the group.

The next step in any algebra book would be to define separable extensions. However, over $\mathbb{Q}$, all extensions are separable and we do not need to

worry about that. A very special role is played by (separable) splitting fields which are then called *finite normal extensions*[24].

Now we are ready to discuss the *Fundamental Theorem of Galois Theory*. The theorem states that if E is a finite normal extension of F then there is a one to one correspondence between intermediate extensions of F and subgroups of $\mathrm{Gal}(E/F)$. The correspondence is the following: to each extension B of F such that $B \leq E$, one associates the largest subgroup G_B of $\mathrm{Gal}(E/F)$ that leaves B fixed. Moreover, B is a finite normal extension of F if and only if G_B is a normal subgroup. In fact, $\mathrm{Gal}(B/F)$ is isomorphic to the factor (or quotient) group $\mathrm{Gal}(E/F)/G_B$.

Let us apply this to our example $E = \mathbb{Q}(2^{1/4}, i)$. As discussed above, E is the splitting field of $z^4 - 2$. It has a basis $\{1, a, a^2, a^3, i, ia, ia^2, ia^3\}$ where $a = 2^{1/4}$.

Since $|E : \mathbb{Q}| = 8$ we must have $|\mathrm{Gal}(E/\mathbb{Q})| = 8$. It is a simple exercise to exhibit the eight automorphisms of E leaving $\mathbb{Q}$ invariant (see section 47.2 of [31]). Studying the composition table one discovers that the group is non-abelian. Moreover, $\mathrm{Gal}(E/\mathbb{Q}) = D_4$, the dihedral group (the symmetry group of a square). If we denote rotations by $k\pi/2$ (with $k = 0, 1, 2, 3$) as ρ_k, mirror images (reflections) as μ_i and diagonal flips as δ_i, then the identification with automorphisms is collected in the table below (only the action on a and i is needed).

	ρ_0	ρ_1	ρ_2	ρ_3	μ_1	δ_1	μ_2	δ_2
$a \rightarrow$	a	$i\,a$	$-a$	$-i\,a$	a	$i\,a$	$-a$	$-i\,a$
$i \rightarrow$	i	i	i	i	$-i$	$-i$	$-i$	$-i$

The lattice of all subgroups of D_4 is well known (see section 47.2 of [31]). According to Galois theory there must be one and only one intermediate extension of $\mathbb{Q}(2^{1/4}, i)$ for each subgroup. This gives rise to the lattice of intermediate extensions of $\mathbb{Q}(2^{1/4}, i)$. Let K_H denote the subfield of $\mathbb{Q}(2^{1/4}, i)$ left fixed by the subgroup H of D_4. For example, it is easy to check that $K_{\{\rho_0, \rho_2\}} = \mathbb{Q}(\sqrt{2}, i)$. Note that $\mathbb{Q}(\sqrt{2}, i)$ is also a splitting field and hence a finite normal extension. One can easily check that $\{\rho_0, \rho_2\}$ is indeed a normal subgroup of D_4! Likewise, consider $K_{\{\rho_0, \mu_1\}} = \mathbb{Q}(2^{1/4})$. This is not a splitting field and one can check that $\{\rho_0, \mu_1\}$ is not a normal subgroup of D_4.

---

[24] The parenthesis around "separable" are there to indicate that it can freely be removed.

Now we can go back to our object of interest: $\text{Gal}(\overline{\mathbb{Q}}/\mathbb{Q})$. Here, we will follow very closely an explanation given in [21] and we will illustrate the main ideas using our example of $\mathbb{Q}(2^{1/4}, i)$. We have already explained the meaning of the algebraic closure of a field. Here, $\overline{\mathbb{Q}}$ is then the algebraic closure of $\mathbb{Q}$, the field of algebraic numbers. This is clearly a complicated object that can be constructed as the union of all splitting fields over $\mathbb{Q}$, which as we know, are finite normal extensions of $\mathbb{Q}$. Let E denote a generic one, then

$$\text{(A.2)} \qquad\qquad \overline{\mathbb{Q}} = \bigcup_{E \in \mathcal{E}} E$$

where $\mathcal{E}$ is the set of all such extensions. For each extension E, we have the corresponding Galois group, $\text{Gal}(E/\mathbb{Q})$, of E over $\mathbb{Q}$.

Consider our favorite example, $E = \mathbb{Q}(2^{1/4}, i)$. Its Galois group over $\mathbb{Q}$ is $\text{Gal}(E/\mathbb{Q}) = D_4$. Consider $L = \mathbb{Q}(\sqrt{2}, i)$. As we saw, $L \leq E$. Now, every automorphism of E leaves L invariant. This is because L is a splitting field. The Galois group of L over $\mathbb{Q}$ is then the factor group $\text{Gal}(L/\mathbb{Q}) = \text{Gal}(E/\mathbb{Q})/\{\rho_0, \rho_2\}$.

Now there is a natural group epimorphism $\rho_{E,L} : \text{Gal}(E/\mathbb{Q}) \to \text{Gal}(L/\mathbb{Q})$ given by the restriction map. That this is an epimorphism, i.e., an onto map, follows from the fact that every automorphism of L that fixes $\mathbb{Q}$ can be extended to an automorphism of E in $|E : L|$ ways. In our example $|E : L| = 2$. Consider the following automorphism of L: $(\sqrt{2}, i) \to (\sqrt{2}, -i)$. This can then be extended to E in two ways a follows: $(2^{1/4}, i) \to (\pm 2^{1/4}, i)$.

Consider now $\mathbb{Q}(i) = K_{\{\rho_0, \rho_1, \rho_2, \rho_3\}}$. This is also a splitting field. We then have the following sequence of finite normal extensions $\mathbb{Q} \leq \mathbb{Q}(i) \leq \mathbb{Q}(\sqrt{2}, i) \leq \mathbb{Q}(2^{1/4}, i)$. From this sequence, we can make an observation that will be very important in the definition of $\text{Gal}(\overline{\mathbb{Q}}/\mathbb{Q})$: an element (g_1, g_2) of the cartesian product $\text{Gal}(\mathbb{Q}(i)/\mathbb{Q}) \times \text{Gal}(\mathbb{Q}(\sqrt{2}, i)/\mathbb{Q})$ can be extended to an element of $\text{Gal}(\mathbb{Q}(2^{1/4}, i)/\mathbb{Q})$ if and only if $\rho_{L, \mathbb{Q}(i)}(g_2) = g_1$. This is because if $g \in \text{Gal}(\mathbb{Q}(2^{1/4}, i)/\mathbb{Q})$ is one of the possible extensions then it has to have a consistent action on each of the subfields.

The absolute Galois group $\text{Gal}(\overline{\mathbb{Q}}/\mathbb{Q})$ can now be constructed in a very similar way. It is a subgroup of the cartesian product of the Galois groups of all finite normal extensions of $\mathbb{Q}$

$$\text{(A.3)} \qquad\qquad \text{Gal}(\overline{\mathbb{Q}}/\mathbb{Q}) < \prod_{E \in \mathcal{E}} \text{Gal}(E/\mathbb{Q})$$

consisting of all elements $(g_{\mathcal{E}}) \in \prod_{E \in \mathcal{E}} \mathrm{Gal}(E/\mathbb{Q})$ (this is an infinite "array" with one entry for each $E \in \mathcal{E}$) satisfying the constraint that $\rho_{K_2, K_1}(g_{K_2}) = g_{K_1}$ whenever $K_1 \leq K_2$. The identification of each $g \in \mathrm{Gal}(\overline{\mathbb{Q}}/\mathbb{Q})$ with the element $(g_{\mathcal{E}})$ implies that g_E is the restriction of g to E. That this set of restrictions is consistent follows from the condition involving ρ.

Finally, the action of g on $\overline{\mathbb{Q}}$ is determined by the action on each finite normal extension via g_E. This is the basic result we used in Section 2.4 where we discussed the action of $\mathrm{Gal}(\overline{\mathbb{Q}}/\mathbb{Q})$ on dessins. We said that if $g \in \mathrm{Gal}(\overline{\mathbb{Q}}/\mathbb{Q})$ then η acts on a dessin by acting on the coefficients of the Belyi map. In other words, the coefficients of the Belyi map, being found as solutions to some set of polynomial equations, belong to a splitting field E and g acts via its restriction g_E.

A.1. Glossary of terms in the text

- An algebraic number is an element $a \in \mathbb{C}$ that generates a finite extension $\mathbb{Q}(a) \geq \mathbb{Q}$.
- $\overline{\mathbb{Q}}$ is the field of all algebraic numbers and it is also the algebraic closure of $\mathbb{Q}$.
- A number field is a finite algebraic extension of $\mathbb{Q}$.
- A monic polynomial is one whose monomial of highest degree has coefficient 1.

Appendix B. The multiplication map as a Belyi-extending map

It was shown in [10, 8] that once a solution to the factorization problem (1.2) is known for $U(N)$, then it is possible to construct a solution to a similar factorization problem for $U(tN)$. Let us first review this construction.

Consider the factorization problem

$$(B.1) \qquad P_t^2(z) - 4\Lambda^{2t} = F_2(z) H_{t-1}^2(z).$$

The solution is given by

$$(B.2) \qquad \begin{aligned} P_t(z) &= 2\Lambda^t \eta^t T_t\left(\frac{z}{2\eta\Lambda}\right), \quad F_2(z) = z^2 - 4\eta^2 \Lambda^2, \\ H_{t-1}(z) &= \eta^{t-1}\Lambda^{t-1} U_{t-1}\left(\frac{z}{2\eta\Lambda}\right), \end{aligned}$$

where $\eta^{2t} = 1$. $T_t(z)$ and $U_{t-1}(z)$ are the Chebyshev polynomials of the first and second kind respectively, defined by setting $z = \cos\theta$ and

(B.3)
$$T_t(z) = \cos(t\theta) \quad U_{t-1}(z) = \frac{1}{t}\frac{dT_t}{dz}(z) = \frac{\sin(t\theta)}{\sin\theta}.$$

This implies that they satisfy the relation

(B.4)
$$1 - T_t^2(z) = (1 - z^2)\, U_{t-1}^2(z).$$

Now suppose we have a solution to the factorization problem

(B.5)
$$P_N^2(z) - 4\Lambda_0^{2N} = F_{2n}(z)H_{N-n}^2(z).$$

Then we can use the solution to (B.2) to construct a solution to

(B.6)
$$P_{tN}^2(z) - 4\Lambda_0^{2tN} = \widetilde{F}_{2n}(z)\widetilde{H}_{tN-n}^2(z)$$

as follows:
(B.7)
$$P_{tN}(z) = 2\Lambda^{tN}\eta^t T_t\left(\frac{P_N(z)}{2\eta\Lambda^N}\right), \quad \widetilde{F}_{2n}(z) = F_{2n}(z),$$

$$H_{tN-n}(z) = \eta^{t-1}\Lambda^{N(t-1)}H_{N-n}(z)\, U_{t-1}\left(\frac{P_N(z)}{2\eta\Lambda^N}\right), \qquad \Lambda_0^{2N} = \eta^2\,\Lambda^{2N}.$$

This procedure to get exactly t solutions to the $U(tN)$ theory from a given solution of the $U(N)$ theory was referred to as the multiplication map (by t) in [5].

Let us now show that the multiplication by t map can be used to construct new Beyi maps from old ones. The simple example of $t = 2$ has already been discussed in Section 4. As discussed in that section, the main point is to use the multiplication map to define the new Belyi map as

(B.8)
$$\widetilde{\beta}_t(z) = 1 - \frac{P_{tN}^2(z)}{4\Lambda_0^{2tN}},$$

where $P_{tN}(z)$ is given by the first equation in (B.7) and $P_N(z)$ gives rise to a Belyi map

(B.9)
$$\beta(z) = 1 - \frac{P_N^2(z)}{4\Lambda_0^{2N}}.$$

We would now like to exhibit (B.8) as the composition of a Belyi-extending map with the Belyi map (B.9). For this purpose, let us define the polynomials

(B.10) $\qquad T_{2k}(z) = M_k(z^2) \qquad$ and $\qquad T_{2k+1}(z) = z\, S_k(z^2)\,.$

This follows from the form of the Chebyshev polynomials (B.3). If we now define the Belyi-extending maps

(B.11) $\alpha_{2k}(u) = 1 - M_k^2(1-u) \qquad$ and $\qquad \alpha_{2s+1}(u) = 1 - (1-u)S_k^2(1-u)\,,$

one can check that

(B.12) $$\widetilde{\beta}_t(z) = \alpha_t(\beta(z))$$

is a Belyi map for all integer values of t. As for α_2, one check that geometrically, the multiplication by t replaces a given edge in a dessin by a branchless tree of length t.

Appendix C. Complete list of trees for $U(6)$

In this appendix, we study the problem of realizing all possible connected trees with six edges. Along the way, we will mention some interesting points about the structure of $\mathcal{N} = 1$ vacua from the matrix model point of view [22].

In Section 5, we studied examples a pure $U(6)$ gauge theory deformed by a cubic superpotential. However, a cubic superpotential does not allow enough flexibility in the non-rigid Seiberg–Witten curve to realize all possible trees with six edges. We mentioned in the text that if we consider a superpotential $W(z)$ of degree $n + 1$, then the curve describing the $\mathcal{N} = 1$ vacua of $U(N)$ is given by

(C.1) $\qquad y^2 = P_N^2(z) - 4\Lambda^{2N} = (W'(z)^2 + f_{n-1}(z))H_{N-n}^2(z)$

where $W'(z)$ has degree n.

However, this is true only for vacua with all values of N_i different from zero. In other words, if $U(N)$ is classically broken to $U(N_1) \times \cdots \times U(N_n)$. It turns out that if $n - s$ of the N_i's are zero then the description of $\mathcal{N} = 1$ vacua is more subtle and it was elucidated in [22] by using matrix model techniques inspired by the Dijkgraaf–Vafa relation [13, 14, 15]. The way to treat all cases at once is by introducing another curve, called the matrix model curve, $y_m^2 = W'(z)^2 + f_{n-1}(z)$. Then, if $U(N)$ is broken classically to

$U(N_1) \times \cdots \times U(N_s)$ the factorization problems to be solved are

(C.2)
$$y^2 = P_N^2(z) - 4\Lambda^{2N} = F_{2s}(z)H_{N-s}^2(z),$$
$$y_m^2 = W'(z)^2 + f_{n-1}(z) = F_{2s}(z)R_{n-s}^2(z).$$

This means in particular, that the $(3,2)$ vacua in Section 5.1 for the $U(6)$ example is the intersection of the $s = 2$ branch with the $s = 1$ branch, where the low-energy gauge groups are $U(1)^2$ and $U(1)$, respectively. This intersection was studied in great generality in [24].

Note, however, that the trivalent and four-valent factorizations in $U(6)$ do not correspond to points, where the $s = 2$ branch intersects the $s = 1$ branch. This is because both values of N_i are nonzero. More generally, it is clear that isolated singular points of a theory with $s = p$ are particular cases of those of a theory with $s = n$ for any $p < n$, since the corresponding branches can intersect.

The set of interesting values of n in the case of $U(6)$ is $n = 1, \ldots, 6$[25]. We now turn to the construction of all possible dessins associated to $U(6)$. It turns out that one only needs to consider a quartic superpotential, i.e., $n = 3$.

Let us prove that $n = 3$ suffices. Instead of starting with $n = 6$ and descending all the way to $n = 3$ it is best to use the fact that isolated singular points give rise to all possible connected trees with six edges. These trees must have seven vertices. All possible valency lists are the following $(6, 0, 0, 0, 0, 1)$, $(5, 1, 0, 0, 1, 0)$, $(5, 0, 1, 1, 0, 0)$, $(4, 2, 0, 1, 0, 0)$, $(4, 1, 2, 0, 0, 0)$, $(3, 3, 1, 0, 0, 0)$ and $(2, 5, 0, 0, 0, 0)$. Recall that a valence list $(u_1, \ldots, u_6)$ means that there are u_k vertices with valence k. These were obtained by requiring that the sum of all u_k's is always seven and that the sum of all u_k's times k is always 12.

The previous valence lists lead to factorization problems of the Seiberg–Witten curve of the form

$$F_6(z)H_1^6(z), \quad F_5(z)Q_1^2(z)H_1^5(z), \quad F_5(z)Q_1^3(z)H_1^4(z),$$
$$F_4(z)Q_2^2(z)H_1^4(z), \quad F_4(z)Q_1^2(z)H_2^3(z), \quad F_3(z)Q_3^2(z)H_1^3(z),$$

and $F_2(z)Q_5^2(z)$, respectively.

---

[25] There is a subtlety when $n = 6$ which is related to the fact that $\mathrm{tr}\Phi^7$ in the superpotential is not an independent quantity but this will not affect our discussion (see [8] for more details).
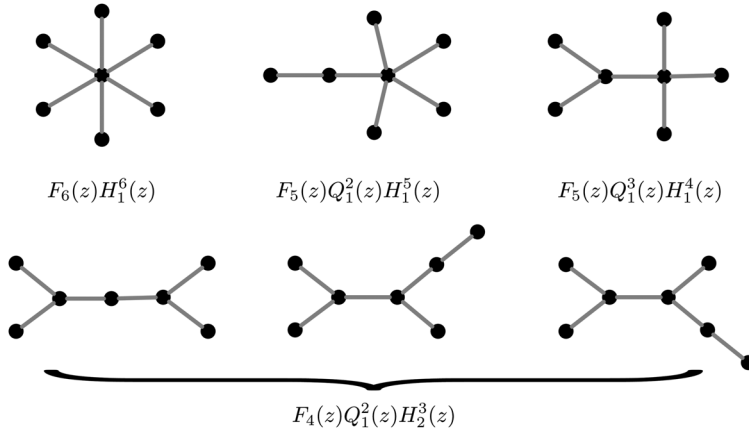
Figure 23: All possible dessins (and the associated factorizations) that appear in the $\mathcal{N} = 2$ moduli space of the $U(6)$ gauge theory, apart from the ones already discussed in the main body of the article. We have omitted the vertices corresponding to the zeroes of $P_6(z)$.

Now we can prove our claim by simple inspection. All these factorization problems are particular points in the space of curves (with $n = 3$) given by

$$(C.3) \qquad y^2 = P_6^2(z) - 4\Lambda^{12} = F_6(z)H_3^2(z) \,.$$

It is also easy to check that $F_6(z)H_1^6(z)$, $F_5(z)Q_1^2(z)H_1^5(z)$, $F_5(z)Q_1^3(z)$ $H_1^4(z)$ and $F_4(z)Q_1^2(z)H_2^3(z)$ cannot possibly be obtained from the cubic superpotential (the $n = 2$ case considered in the text), while all other factorizations — $F_4(z)Q_2^2(z)H_1^4(z)$, $F_3(z)Q_3^2(z)H_1^3(z)$ and $F_2(z)Q_5^2(z)$ — were considered in Section 5.

The inherently $n = 3$ factorizations give rise to only six different trees (figure 23).

References

[1] N. Seiberg and E. Witten, *Electric — magnetic duality, monopole condensation, and confinement in N = 2 supersymmetric Yang-Mills theory*, Nucl. Phys. B **426** 19 (1994), [Erratum-ibid. B **430** (1994), 485], hep-th/9407087.

[2] N. Seiberg and E. Witten, *Monopoles, duality and chiral symmetry breaking in N = 2 supersymmetric QCD*, Nucl. Phys. B **431** (484) (1994), hep-th/9408099.

[3] E. Witten, *Monopoles and four manifolds*, Math. Res. Lett. **1** (769) (1994), hep-th/9411102.

[4] G. W. Moore and N. Seiberg, *Polynomial equations for rational conformal field theories*, Phys. Lett. B **212** (1988), 451.

[5] G. W. Moore and N. Seiberg, *Naturality in Conformal Field Theory*, Nucl. Phys. B **313** (1989), 16.

[6] G. W. Moore and N. Seiberg, *Classical and quantum Conformal Field Theory*, Commun. Math. Phys. **123** (1989), 177.

[7] A. Grothendieck, *Esquisse d'un Programme*, Preprint, 1985. Reprinted with English translation in *Geometric Galois Actions*, Edited by L. Schneps and P. Lochak, London Mathematical Society Lecture Notes Series, **242**, 1997, Cambridge University Press, Cambridge, England.

[8] F. Cachazo, N. Seiberg and E. Witten, *Phases of N = 1 supersymmetric gauge theories and matrices*, JHEP **0302** (2003), 042, hep-th/0301006.

[9] F. Cachazo, N. Seiberg and E. Witten, *Chiral rings and phases of supersymmetric gauge theories*, JHEP **0304** (2003), 018, hep-th/0303207.

[10] F. Cachazo, K. A. Intriligator and C. Vafa, *A large N duality via a geometric transition*, Nucl. Phys. B **603** (2001), 3, hep-th/0103067.

[11] F. Cachazo and C. Vafa, *N = 1 and N = 2 geometry from fluxes*, arXiv:hep-th/0206017.

[12] M. R. Douglas and S. H. Shenker, *Dynamics of SU(N) supersymmetric gauge theory*, Nucl. Phys. B **447** (1995), 271, hep-th/9503163.

[13] P. C. Argyres and M. R. Douglas, *New phenomena in SU(3) supersymmetric gauge theory*, Nucl. Phys. B **448** (1995), 93, hep-th/9505062.

[14] G.V. Belyi, *On Galois extensions of a maximal cyclotonic field*, Math. U.S.S.R. Izvestija **14** (1980), 247–256.

[15] L. Schneps, *The Grothendieck Theory of Dessins d'Enfants*, London Mathematical Society Lect. Note Series, **200**, 1994.

[16] S.K. Ashok, F. Cachazo and E. Dell'Aquila, *Strebel differentials with integral lengths and Argyres–Douglas singularities*, hep-th/0610080.

[17] A. Hanany and Y. Oz, *On the quantum moduli space of vacua of $N = 2$ supersymmetric $SU(N(c))$ gauge theories*, Nucl. Phys. B **452** (1995), 283, hep-th/9505075.

[18] P.C. Argyres, M.R. Plesser and A.D. Shapere, *The Coulomb phase of $N = 2$ supersymmetric QCD*, Phys. Rev. Lett. **75** (1995), 1699, hep-th/9505100.

[19] G. Shabat and A. Zvonkin, *Plane Trees and Algebraic Numbers*, in Jerusalem Combinatorics '93, **178**, AMS Publications, R.I., USA.

[20] M. Wood, *Belyi-extending maps and the Galois action on dessins d'enfants*, math.NT/0304489.

[21] G. Jones and M. Streit, *Galois groups, monodromy groups and cartographic groups geometric galois actions: 2. the inverse galois problem, moduli spaces and mapping class groups*, London Math. Soc. Lect. Notes Series, **243**, Cambridge Univ. Press, Cambridge, England, 1997, 25–65.

[22] F. Cachazo, M. R. Douglas, N. Seiberg, and E. Witten, *Chiral rings and anomalies in supersymmetric gauge theory*, JHEP **0212** 071 (2002), hep-th/0211170.

[23] T. Eguchi and Y. Sugawara, *Branches of $\mathcal{N} = 1$ Vacua and Argyres–Douglas Points*, JHEP **0305**: (2003), 063, hep-th/0305050.

[24] D. Shih, *Singularities of $N = 1$ supersymmetric gauge theory and matrix models*, JHEP **0311** (2003), 025, hep-th/0308001.

[25] A. Kapustin, *The Coulomb branch of $N = 1$ supersymmetric gauge theory with adjoint and fundamental matter*, Phys. Lett. B **398** (1997), 104, hep-th/9611049.

[26] N. Seiberg, *Adding fundamental matter to "Chiral rings and anomalies in supersymmetric gauge theory"*, JHEP **0301** (2003), 061, hep-th/0212225.

[27] V. Balasubramanian, B. Feng, M. X. Huang and A. Naqvi, *Phases of $N = 1$ supersymmetric gauge theories with flavors*, Annals Phys. **310** (2004), 375, hep-th/0303065.

[28] R. Dijkgraaf and C. Vafa, *Matrix models, topological strings, and supersymmetric gauge theories*, Nucl. Phys. B **644** (2002), 3, hep-th/0206255.

[29] R. Dijkgraaf and C. Vafa, *On geometry and matrix models*, Nucl. Phys. B **644** (2002), 21, hep-th/0207106.

[30] R. Dijkgraaf and C. Vafa, *A perturbative window into non-perturbative physics*, hep-th/0208048.

[31] John B. Fraleigh, *First Course in Abstract Algebra*, 3rd Ed., Addison-Welsley, Reading, Mass.

PERIMETER INSTITUTE FOR THEORETICAL PHYSICS
WATERLOO, ONTARIO,
ON N2L 2Y5, CANADA
E-mail address: `sashok@perimeterinstitute.ca`
E-mail address: `fcachazo@perimeterinstitute.ca`

NHETC, DEPARTMENT OF PHYSICS
RUTGERS UNIVERSITY
136, FRELINGHUYSEN ROAD,
PISCATAWAY, NJ 08854, USA
E-mail address: `dellaqui@physics.rutgers.edu`